



uOttawa

L'Université canadienne  
Canada's university

**FACULTÉ DES ÉTUDES SUPÉRIEURES  
ET POSTDOCTORALES**



**uOttawa**

L'Université canadienne  
Canada's university

**FACULTY OF GRADUATE AND  
POSTDOCTORAL STUDIES**

**Kim Lesage**

-----  
AUTEUR DE LA THÈSE / AUTHOR OF THESIS

**M.A.Sc. (Civil Engineering)**

-----  
GRADE / DEGRÉ

**Department of Civil Engineering**

-----  
FACULTÉ, ÉCOLE, DÉPARTEMENT / FACULTY, SCHOOL, DEPARTMENT

**Experimental studies of thaw consolidation of fine grained frozen soils from the Mackenzie Valley**

-----  
TITRE DE LA THÈSE / TITLE OF THESIS

**Dr. Baolin Wang**

-----  
DIRECTEUR (DIRECTRICE) DE LA THÈSE / THESIS SUPERVISOR

-----  
CO-DIRECTEUR (CO-DIRECTRICE) DE LA THÈSE / THESIS CO-SUPERVISOR

**EXAMINATEURS (EXAMINATRICES) DE LA THÈSE / THESIS EXAMINERS**

**Dr. Paul Simms**

**Dr. Mamadou Fall**

**Dr. Erman Evgin**

**Gary W. Slater**

-----  
Le Doyen de la Faculté des études supérieures et postdoctorales / Dean of the Faculty of Graduate and Postdoctoral Studies

# **Experimental studies of thaw consolidation of fine grained frozen soils from the Mackenzie Valley**

**Kim Lesage**

Thesis submitted to the  
Faculty of Graduate and Postdoctoral Studies  
In partial fulfillment of the requirements for the degree of

**MASTER OF APPLIED SCIENCE**

in Civil Engineering



Ottawa-Carleton Institute for Civil Engineering  
University of Ottawa  
Ottawa, Canada



Library and Archives  
Canada

Published Heritage  
Branch

395 Wellington Street  
Ottawa ON K1A 0N4  
Canada

Bibliothèque et  
Archives Canada

Direction du  
Patrimoine de l'édition

395, rue Wellington  
Ottawa ON K1A 0N4  
Canada

*Your file* *Votre référence*  
ISBN: 978-0-494-59874-0  
*Our file* *Notre référence*  
ISBN: 978-0-494-59874-0

**NOTICE:**

The author has granted a non-exclusive license allowing Library and Archives Canada to reproduce, publish, archive, preserve, conserve, communicate to the public by telecommunication or on the Internet, loan, distribute and sell theses worldwide, for commercial or non-commercial purposes, in microform, paper, electronic and/or any other formats.

The author retains copyright ownership and moral rights in this thesis. Neither the thesis nor substantial extracts from it may be printed or otherwise reproduced without the author's permission.

**AVIS:**

L'auteur a accordé une licence non exclusive permettant à la Bibliothèque et Archives Canada de reproduire, publier, archiver, sauvegarder, conserver, transmettre au public par télécommunication ou par l'Internet, prêter, distribuer et vendre des thèses partout dans le monde, à des fins commerciales ou autres, sur support microforme, papier, électronique et/ou autres formats.

L'auteur conserve la propriété du droit d'auteur et des droits moraux qui protègent cette thèse. Ni la thèse ni des extraits substantiels de celle-ci ne doivent être imprimés ou autrement reproduits sans son autorisation.

---

In compliance with the Canadian Privacy Act some supporting forms may have been removed from this thesis.

While these forms may be included in the document page count, their removal does not represent any loss of content from the thesis.

Conformément à la loi canadienne sur la protection de la vie privée, quelques formulaires secondaires ont été enlevés de cette thèse.

Bien que ces formulaires aient inclus dans la pagination, il n'y aura aucun contenu manquant.

  
**Canada**

# Table of Contents

List of Tables.....	iv
List of Figures.....	v
Legend .....	viii
Abstract.....	ix
Résumé.....	ix
Acknowledgments .....	xi
1 Introduction .....	1
1.1 General .....	1
1.2 Thawing and pore water pressure.....	5
1.3 Statement of the problem.....	7
1.4 Objectives of the investigation .....	9
1.5 Scope of the investigation .....	10
1.6 Thesis outline.....	10
2 Literature review.....	12
2.1 Thaw consolidation theory .....	12
2.2 Experimental studies on pore pressure.....	16
2.3 Summary.....	20
3 Laboratory Testing .....	21
3.1 Description of laboratory apparatus .....	21
3.2 Description of sample .....	27
3.3 Testing Procedure.....	28
3.4 Laboratory results .....	30
3.4.1 Temperature .....	31
3.4.2 Pore water pressure.....	34
3.4.2.1 Sensor calibration .....	35
3.4.2.2 Test data .....	36
3.4.3 Soil moisture change .....	37
4 Numerical modelling.....	39
4.1 Thermal modelling using Temp/W .....	39
4.1.1 Model descriptions and boundary conditions .....	39

4.1.2	Material properties .....	42
4.1.3	Results.....	47
4.2	Moisture modelling using Vadose/W .....	48
4.2.1	Model descriptions and boundary conditions.....	49
4.2.2	Material properties .....	50
4.2.3	Results.....	53
5	Analysis.....	55
5.1	Thermal behaviour .....	56
5.1.1	Analysis .....	56
5.1.2	Derived thermal properties of soil samples.....	58
5.2	Pore water pressure.....	60
5.2.1	Pore water pressure generation with respect to the thaw front.....	60
5.2.2	Pore water pressure changes .....	62
5.2.2.1	Pore pressures at 30 cm depth .....	62
5.2.2.2	Pore pressures at 50 cm depth .....	66
5.2.3	Remarks on accuracy of measured data .....	67
5.2.4	Comparison of pore pressure data with theoretical results .....	68
5.3	Moisture migration .....	70
6	Conclusion .....	73
	References.....	75
	Appendix A – Thaw consolidation theory .....	84

## List of Tables

Table 4.1 Climate data applied as surface boundary condition .....	41
Table 4.2 Atterburg limits .....	42
Table 4.3 Soil parameters determined before the freezing process .....	42
Table 4.4 Silty clay soil parameters determined from the literature .....	43
Table 4.5 Volumetric heat capacity and water content.....	45
Table 4.6 Material properties used for the Vadose/W analysis .....	51
Table 5.1 Thermal constant determination .....	59

## List of Figures

Figure 1.1 Permafrost coverage in Canada (after Geological Survey of Canada, 2007) .....	2
Figure 1.2 Global mean surface temperatures from 1856 to 2005 (from Global warming art, 2007, after Houghton et al., 2001) .....	3
Figure 1.3 Reduction in volume due to excess pore water dissipation .....	6
Figure 2.1 One-dimensional thaw consolidation configuration (after Morgenstern and Nixon, 1971) .....	13
Figure 2.2 Distribution of the normalized excess pore pressures for various thaw consolidation ratios when the soil is consolidated by its own weight	16
Figure 3.1 Thaw consolidation laboratory equipment .....	22
Figure 3.2 Profile view of the silty clay/insulation system setup .....	23
Figure 3.3 Steel base of the column open to cold room temperature .....	23
Figure 3.4 Location of the pressure and temperature sensors .....	24
Figure 3.5 Tip of the PDCR-81 miniature pore pressure transducer (after Muraleetharan and Granger, 1999) .....	25
Figure 3.6 Mounting of the 4 silicone heaters in the lid .....	26
Figure 3.7 Completed thaw-consolidation device .....	26
Figure 3.8 Typical grain size distribution (after Su et al., 2006).....	27
Figure 3.9 Freezing of fine-grained permafrost samples .....	28
Figure 3.10 Experimental temperature results during thawing of sample #1 and #2 .....	32
Figure 3.11 Cold room and heating chamber temperatures during freezing and thawing .....	33
Figure 3.12 Experimental temperature results during thawing of sample #3.....	34
Figure 3.13 Calibration of pore pressure sensors .....	35
Figure 3.14 Experimental pore water pressure results during thawing of sample #3 .....	36
Figure 3.15 Excess pore water pressure results during thawing of sample #3...	37

Figure 3.16 Gravimetric water content for samples #1, #2 and #3 at different depths, following the thawing process .....	38
Figure 4.1 Finite element mesh constructed for thermal analysis .....	40
Figure 4.2 Range of coefficient of consolidation for silts and clays (after U.S. Department of the Navy, 1971).....	44
Figure 4.3 Comparison of the computed coefficient of consolidation for various clays (after Terzaghi et al., 1996) .....	45
Figure 4.4 Thermal conductivity function used in the analysis .....	46
Figure 4.5 Unfrozen volumetric water content function used in the analysis .....	46
Figure 4.6 Soil temperatures with time predicted by the Temp/W model for the case where the soil is fully insulated along lateral boundaries .....	47
Figure 4.7 Soil temperatures with time predicted by the Temp/W model for the case where the soil is not insulated along lateral boundaries.....	48
Figure 4.8 Finite element mesh constructed for Vadose/W analysis .....	50
Figure 4.9 Volumetric water content function for silty clay.....	51
Figure 4.10 Hydraulic conductivity function for silty clay .....	52
Figure 4.11 Volumetric water content with time predicted by the Vadose/W model based on a saturated hydraulic conductivity of $10^{-5}$ cm/s .....	53
Figure 4.12 Volumetric water content with time predicted by the Vadose/W model based on a saturated hydraulic conductivity of $10^{-7}$ cm/s .....	54
Figure 5.1 Coupled processes in a soil matrix (after Fall, 2007) .....	55
Figure 5.2 Thawing temperature envelope and results for samples #1 and #2 after 16 days of thawing .....	57
Figure 5.3 Thawing temperature envelope and results for sample #3 after 29 days of thawing.....	58
Figure 5.4 Thaw rate for two different depths.....	61
Figure 5.5 Temperature and pore water pressure readings at 30 cm depth from day 2 to day 5 of the laboratory testing.....	62
Figure 5.6 Pore water pressures at 30 cm depth.....	63
Figure 5.7 Temperature and pressure recorded during soil freezing and thawing test (after Harris and Davies, 1998).....	64

Figure 5.8 Experimental pore water pressure results for sample #3 at a depth of 30 cm.....	64
Figure 5.9 Pore water pressures at 50 cm from soil surface .....	66
Figure 5.10 Theoretical and experimental excess pore water pressure .....	69
Figure 5.11 Experimental and theoretical moisture contents after 16 days of thawing .....	70
Figure 5.12 Experimental and theoretical moisture migration after 29 days of thawing .....	71

## Legend

$C$	= Volumetric heat capacity (kJ/m <sup>3</sup> /°C)
$c_v$	= coefficient of consolidation
$e$	= Void ratio
$erf()$	= error function
$G_s$	= Specific gravity
IPCC	= Intergovernmental Panel on Climate Change
$k$	= Hydraulic conductivity (cm/s)
$m_v$	= Coefficient of consolidation (cm <sup>2</sup> /s)
$P_0$	= load applied to the surface
$R$	= thaw consolidation ratio
$S$	= Degree of saturation
$t$	= time
$u$	= excess pore pressure
$w$	= Gravimetric water content (%)
$Wl$	= Liquid limit
$Wp$	= Plastic limit
$Wn$	= Natural water content
$x$	= depth measured from the ground surface
$X$	= depth to the thaw plane
$\alpha$	= thermal constant determined in the solution of the heat conduction problem
$\gamma$	= Unit weight (kN/m <sup>3</sup> )
$\gamma_d$	= Dry unit weight (kN/m <sup>3</sup> )
$\gamma'$	= submerged unit weight of the soil
$\theta$	= Volumetric water content
$\lambda$	= Thermal Conductivity (kJ/day/m/°C)

## **Abstract**

A study was conducted on the thaw consolidation behaviour of fine grained permafrost soils, which are commonly found in the Mackenzie Valley, Canada. In 1971, Morgenstern and Nixon proposed a thaw consolidation theory. A laboratory study has been carried out with a focus on the consolidation behaviour of thawing fine grained permafrost soils for a case where the thawing soil consolidates under its own weight. Numerical modelling was carried out to predict the temperature behaviour and moisture migration observed in the laboratory. The design of the laboratory apparatus is discussed and the results are evaluated in comparison with the numerical and theoretical predictions. The finite element software are proved useful in predicting the soil thermal and hydraulic behaviour. Although the laboratory results and that from the thaw consolidation theory developed by Morgenstern and Nixon (1971) cannot be compared directly due to many uncertainties, the laboratory results are in reasonable agreement.

## **Résumé**

En 1971, Morgenstern et Nixon ont avancé une théorie sur la consolidation des sols lors du dégel. Une étude en laboratoire a été conduite en mettant l'accent sur le comportement de consolidation du pergélisol à grains fins durant le dégel lorsque le sol qui dégèle est consolidé par son propre poids. De la modélisation numérique a été réalisée pour prédire le comportement de consolidation du pergélisol. La conception de l'appareil de laboratoire est examinée et les résultats sont évalués en comparaison avec les prédictions numériques et théoriques. Le logiciel de modélisation numérique s'est avéré utile pour prédire le comportement thermique et hydraulique du pergélisol. Malgré le fait que les résultats obtenus en laboratoire et ceux obtenus en vertu de la théorie développée par Morgenstern et Nixon (1971) ne peuvent être comparés

directement à cause des nombreuses incertitudes, les résultats de laboratoire sont raisonnablement comparable aux résultats théoriques.

## **Acknowledgments**

A very special thank you to Dr. B. Wang for sharing his love of geotechnical engineering with me. And many thanks for his continued guidance and valuable criticism throughout the research project, for helping me with the interpretation of the data and for helping me improve the quality of my work. Also, thank you for giving me the great opportunity of going to Inuvik, it was an experience of a lifetime.

Many thanks to GSC Northern Canada for the use of their laboratory and cold room facilities and for the funding of this research. Thank you to my colleagues for their valuable advice and also for getting full of “mud” when help was needed!

Many thanks to Kenneth Lalonde and all the men at CANMET - Ottawa for building the laboratory equipment and helping with the design.

Thank you to my fellow students and to my professors at the University of Ottawa, in particular Dr. Vanapalli and Dr. Fall, for their encouragement and for always making me feel like part of your team.

Thank you to Greg Newman of Geo-Slope International for always promptly replying to my e-mails and helping me develop my numerical models to best represent the laboratory program.

Thank you to Nicole and grand-papa for your confidence in me and for proof-reading many of my papers and always providing me with valuable suggestions and encouragement.

Thank you to my family and a special thank you to my husband for their continued support and encouragement. And finally, thank you to my mother and father for always believing in me.

# 1 Introduction

The area of this research is the field of cold region engineering. With a combination of climate change and an increasing demand for construction as well as oil and gas development in cold regions, there is a need for a better understanding of permafrost behaviour when thawing. Further knowledge of this process will allow engineers to find the most suitable solutions when dealing with geotechnical hazards and major problems that arise when soil thawing occurs in permafrost regions, such as landslides and thaw settlement.

This study examines the thaw consolidation behaviour of fine grained soil samples from permafrost ground from the Mackenzie Valley, Canada.

## 1.1 General

The Mackenzie valley is located in the Northwest Territories, Canada. Permafrost underlies more than 50% of the ground surface in Canada (Johnston, 1981) and underlies most of the Mackenzie valley (Aylsworth et al., 2000). Permafrost is defined as “the thermal condition in soil or rock of having temperatures below 0°C persist over at least two consecutive winters and the intervening summer” (Brown and Kupsch, 1974). There are two major divisions of permafrost, namely continuous permafrost and discontinuous permafrost, as shown in Figure 1.1. For permafrost to persist, the freezing index (degree days below 0°C) must generally be greater than the thawing index (degree days above 0°C) (Dyke, 2000). Furthermore, the depth of permafrost varies from very thick near the north (>100 m) to thin in the extreme south (<5 m) (Aylsworth et al., 2000). Overlying permafrost, there often lies an “active layer” that annually thaws in the spring/summer and freezes in the fall/winter. The thickness of the active layer is dependant on climate, vegetation, geomorphology, hydrology and the permafrost soil properties (Nixon, 2000). Deposits of ground moraine (till)

are most commonly found in the Mackenzie valley and also underlie many other surficial sediments (Aylsworth et al., 2000).

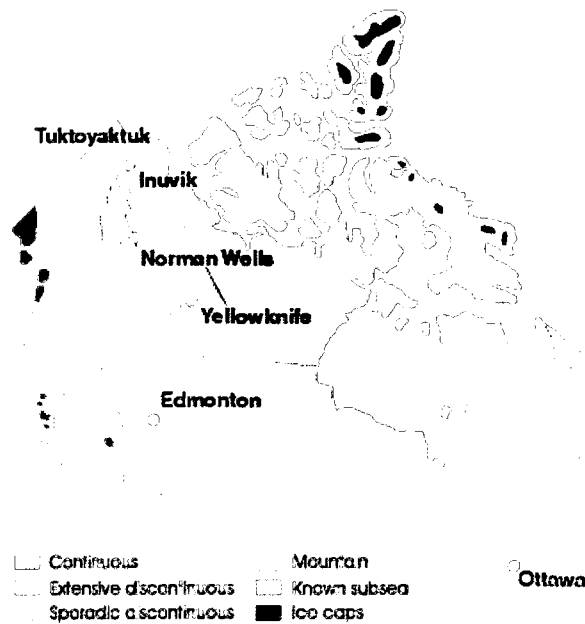


Figure 1.1 Permafrost coverage in Canada (after Geological Survey of Canada, 2007)

Recent proposals to develop natural gas fields in the Mackenzie Delta have triggered a need for further understanding of the freezing and thawing processes in permafrost soils. Thawing of permafrost is a major problem for construction purposes in areas of continuous and discontinuous permafrost. In pipeline construction, the phenomenon of thawing can be associated with many things, such as heat transfer from oil in the pipelines, clearing or disturbance of vegetation in the pipeline right-of-way, construction equipment activity or placement of an embankment over an organic layer (Nelson et al. 1983, Nixon and Pick, 1985). Forest fires and climate change (i.e. high summer temperatures and high precipitation) must also be taken into consideration during pipeline design and construction in permafrost zones.

There is a concern that global warming, or climate change, may accelerate the degradation of permafrost, consequently triggering an increased number of

landslides. As shown in Figure 1.2, global surface temperatures are on the rise. From this data, scientists at Cambridge University have calculated that the global average near-surface temperature has increased by approximately  $0.60 \pm 0.2^\circ\text{C}$  since 1856 (Houghton et al. 2001). These scientists have also computed a warming rate of  $0.17^\circ\text{C}$  per decade since 1976. According to the 2007 Intergovernmental Panel on Climate Change (IPCC), a warming of about  $0.2^\circ\text{C}$  per decade is projected for the next two decades (IPCC 2007). Moreover, climate scientists from around the world have established that average global temperatures could increase by 1.4 to 5.8 degrees Celsius by the end of this century (Government of Canada, 2004). With these projections in mind, it is evident that the increase in global temperature from one year to another cannot be predicted with certainty. However we can definitely expect a slow decrease in both the extent and thickness of permafrost in the Mackenzie Valley due to the projected warming trend.

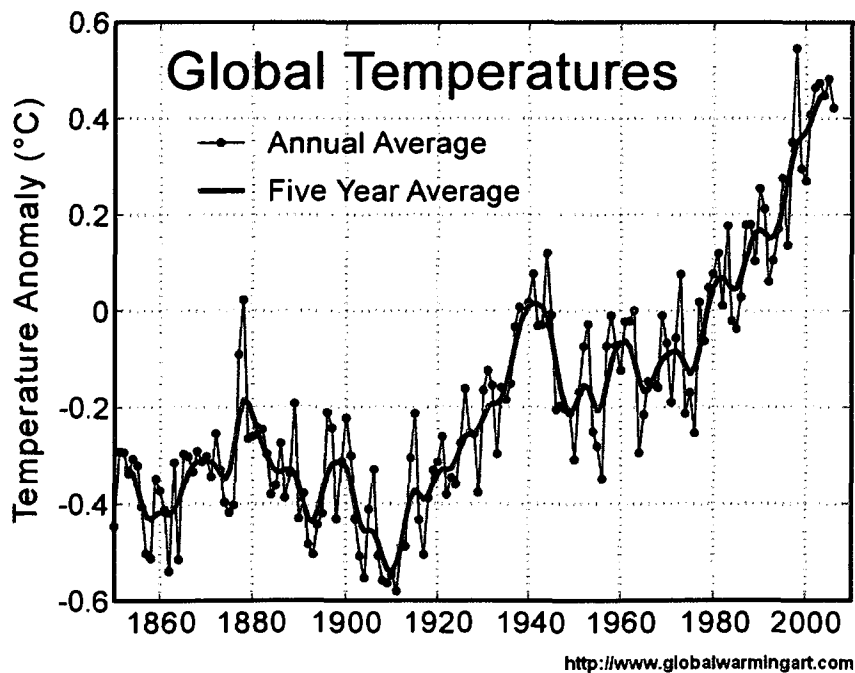


Figure 1.2 Global mean surface temperatures from 1856 to 2005 (from Global warming art, 2007, after Houghton et al., 2001)

There are numerous problems associated with thawing of permafrost soils. If there are buildings or structures constructed over the soil, they may settle or even collapse if the settlement is not evenly distributed. Differential settlement might also occur where a pipeline has been installed, causing the pipes to break or leak. Landslides may be triggered if the thaw boundary reaches the permafrost soil and excess pore water pressures are generated, causing a decrease in the internal shear strength of the soil.

For engineers, one of the most important problems that arises from thawing of permafrost is landslides. Hence, assessing the stability of either naturally occurring permafrost slopes, or of new slopes formed by earthworks, is of great and obvious importance in the field of civil engineering in cold regions, particularly geotechnical engineering. In 2000, approximately 3400 landslides had been mapped in the Mackenzie Valley (Aylsworth et al., 2000). Although some of these landslides are the result of river erosion, many are related to thermal changes in the ground and thawing of permafrost. In cohesive soils, such as silty clay found in the Mackenzie Valley which are usually ice-rich, the thawing material behaves as a fluid, thus producing a landslide. Thawing of permafrost is a very important process to understand in order to minimize the amount of landslides occurring in the Mackenzie Valley and to develop new methods of permafrost slope control.

A landslide may be triggered if thawing depths exceed the active layer and penetrate in to the permafrost, thus decreasing its shear strength. When a landslide takes place, the underlying permafrost is exposed to the atmosphere. The warm summer months will cause the underlying ice to melt, thus inducing continued thawing and retrogressive landslides, year after year. It is essential to understand the thawing processes in order to prevent such landslides from occurring.

Based on field investigations and previous research, researchers have found that there is a transient layer between the active layer and the permafrost layer (Shur et al., 2005, Wang et al., 2005). The active layer is subjected to annual freeze-thaw cycles; however, the depth of thaw is highly variable. Because of annual weather fluctuations, there is a part of the permafrost that will undergo occasional freeze-thaw cycles without causing slope failure. This describes the transient layer - a transition zone between the active layer and the underlying permafrost layer. The transient layer is a relatively new concept that is important in landslide and slope stability analysis seeing that landslides may occur if the thaw line exceeds the transient zone and penetrates the ice-rich permafrost (Wang and Lesage, 2007).

Finally, when permafrost soils thaw, a significant amount of water and pore pressures are generated, which may induce a landslide. Landslides that are caused by excess pore water pressures are commonly found in the fine-grained permafrost soils of the Mackenzie valley. This following section will review the concepts of thawing of permafrost soils and related pore water pressures.

## ***1.2 Thawing and pore water pressure***

When fine-grained soils freeze, ice in the form of ice lenses is accumulated in the soil, causing it to heave (Saarelainen, 1999). When the ice in the soil thaws, the resulting water is liberated and drains out, causing further volume change in the soil. Due to thawing of the soil, there is “an excess pore pressure setup relative to the final independent pore pressure state” (Lee et al., 1983). Excess pore pressures are defined as “the amount by which the pore water pressure exceeds the equilibrium pore pressure” (USACE, 1995). Thus, when the ice in the soil thaws, excess pore pressures are generated due to subjected loading caused by the soils self-weight or a combination of self-weight and applied load (Konrad and Roy, 2000). The pore pressures will dissipate and the soil will consolidate until hydrostatic pore pressures are established in the soil element,

which is illustrated in Figure 1.3. Warming and thawing, or thermal degradation, of fine-grained permafrost may possibly lead to thaw consolidation. This phenomenon can be described as a volume reduction or change in void ratio resulting in settlement of frozen soils that are rich in ice, during a thawing period.

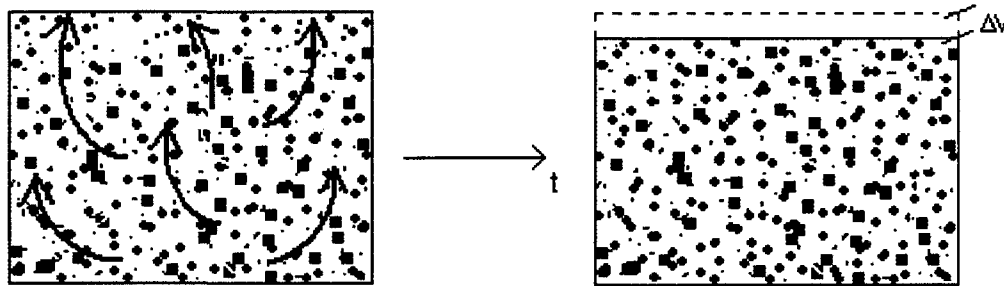


*Figure 1.3 Reduction in volume due to excess pore water dissipation*

The rate of settlement and consolidation during thaw is dependant on the rate of excess pore water dissipation, therefore on the amount and distribution of ice in the soil (Banerjee and Datta, 1991, Luscher and Afifi-Sherif, 1973). If thawing occurs at a slow rate, settlement may proceed concurrently with thawing. However, if thawing occurs at rate higher than the discharge capacity of the soil, excess pore pressures can be generated and have severe implications.

The consolidation behaviour of a soil depends on many factors, including the physical properties of the soil, moisture supply, amount and distribution of the ice in the soil, precipitation, load, etc. Almost all moisture located in permafrost occurs in the form of ice. Higher ice content in the soil will result in a higher amount of thaw consolidation, thus a greater amount of settlement. If thawing is occurring at a fast rate, the pore water may not drain as quickly as it is generated, thus causing excess pore water pressures to build up within the soil (Morgenstern and Nixon, 1971). This is often the case with silts and clays since they have low coefficients of permeability. Thaw consolidation of fine-grained soils may lead to an increase in the excess pore pressures as well as a decrease in the shear strength, bearing capacity and stability of the soil (Nixon,

1973, Wu and Tong, 1991, Harris et al., 2001, Williams and Smith, 1991). Slopes may become unstable and differential settlement may be aggravated. Thus it is important for engineers to understand the processes that occur during thawing of permafrost soils. It has been calculated that soils most sensitive to thaw settlement are moraine, fine-grained lacustrine and organic bog (Aylsworth et al., 2000). These geological materials are commonly found in the Mackenzie Valley, thus making this area susceptible to landslides and thaw settlement problems.

### **1.3 Statement of the problem**

Thawing of an ice-rich soil causes a reduction in void ratio, which is why this process is referred to as thaw consolidation. Many engineering applications in permafrost regions require thaw consolidation theory for proper design, analysis and mitigation; therefore it is imperative to verify its every detail. The permafrost region of interest for this research project is the Mackenzie valley, Northwest Territories, Canada. This region was selected as extensive investigations are presently being carried out by the Geological Survey of Canada to better comprehend the failure mechanism and triggers of landslides of this northern area. The results of these investigations will lead to an improvement of the landslide prevention measures that are presently being proposed for the potential oil and gas development project in the Mackenzie valley.

Silty clay is commonly found in the Mackenzie valley. There are numerous landslides in such fine-grained permafrost soils. Thus it is of interest to verify the engineering behaviour of thawing fine-grained permafrost soils from the Mackenzie valley for this research project.

The key interest of this research is about pore water pressures in thawing permafrost soils. Theories of soil mechanics and of thaw consolidation are essential when designing structures and numerous mitigation means in ice-rich

permafrost areas. Thus it is very important that the equations and knowledge these engineers are using for their planning and designs are accurate and up-to-date in order to minimize all risks of failure.

In 1971, Morgenstern and Nixon developed a thaw consolidation theory. Excess pore water pressures and settlements were calculated for two loading conditions: a weightless material and for a soil consolidating under its own weight. Through the years, the thaw-consolidation theory that was developed by Morgenstern and Nixon has been investigated. However, no researcher has verified the thaw-consolidation behaviour for a case where the thawing soil is consolidated by its own weight. It is known that excess pore water pressures increase linearly with increasing depth. This study evaluates if this is the case for a thawing silty clay soil.

In order to best represent the thawing behaviour of the fine-grained permafrost soils found in the Mackenzie valley, the samples used for the laboratory experiment must be prepared with the most suitable moisture content. It has been established that a landslide may be triggered if thawing depths penetrate in to the ice-rich permafrost soil. Hence, it is of interest to represent the average moisture content found in ice-rich permafrost soils during the laboratory analysis. Based on recent field investigations, an average moisture content of 40% by weight has been measured near the surface of the permafrost layer. Using this particular moisture content will allow engineers to predict and have a better understanding of the behaviour of the permafrost when thawing. Thus, the most suitable prevention measures or remedial actions will be established while performing slope stability analysis in periglacial environments which may be subjected to thawing.

In addition, small samples have always been used in past laboratory experiments of this type. Morgenstern and Smith (1972) developed a laboratory model "Permode" to assess the validity of the thaw consolidation theory using

samples of 32.3 mm in height. Eigenbrod et al. (1996) measured pore water pressures in samples of 70 mm in height. And Harris et al. (1995) tested samples of 300 mm in height while modelling periglacial solifluction. Due to size effect, the results from the small samples could be more effected by the applied boundary conditions. Therefore, it is in our interest to analyze the behaviour of temperature, moisture migration and pore water pressure of fine grained soil samples in a larger scale.

#### **1.4 Objectives of the investigation**

The objectives of the thesis are related to thawing of permafrost soils in the Mackenzie valley, Canada.

The main objective is to verify the thaw-consolidation theory developed by Morgenstern and Nixon (1971) for a case where the thawing soil is consolidated by its own weight. The temperature, pore water pressure and moisture migration behaviour of a thawing fine-grained ice-rich permafrost soil from the Mackenzie valley will be verified through a large-scale laboratory program. Furthermore, numerical models will be developed to predict the temperature variation and moisture migration occurring during the thawing process in order to assess the effectiveness of the laboratory device to represent natural permafrost thawing.

Thaw consolidation is highly complex due to the coupled mechanical, thermal and hydraulic processes occurring throughout the soil matrix. Due to limitations of time and equipment, this study is limited to verifying the experimental pore water pressure results in comparison to the thaw consolidation theory, and to the comparison of the temperature and moisture behaviour obtained from the experimental and numerical analysis.

## **1.5 Scope of the investigation**

This research focuses on the behaviour of pore water pressure, moisture migration and temperature in a thawing fine-grained permafrost soil.

For the purpose of this research, a laboratory device has been developed to examine the thaw consolidation behaviour of permafrost soil. A laboratory program was setup to verify the consolidation behaviour of fine grained permafrost samples from the Mackenzie Valley, Canada, for a case where the thawing soil is consolidated by its own weight. Freezing and heating systems were setup and carefully designed to simulate thawing conditions that would occur in the Mackenzie Valley. The results of the laboratory programs are compared with theoretical and numerical predictions.

The theoretical predictions were established based on the thaw consolidation theory developed by Morgenstern and Nixon in 1971. As for the numerical predictions, these were determined from finite element models designed to represent the laboratory model. The numerical modelling was carried out using Temp/W and Vadose/W, which are finite element software developed by Geo-Slope International (Geo-Slope International Ltd., 2007).

## **1.6 Thesis outline**

A literature review is presented in Chapter 2, including the thaw consolidation theory and previous research on pore water pressure that has motivated this study.

Chapter 3 presents in detail the laboratory program that was developed to observe the thaw consolidation behaviour of fine-grained permafrost soils. The laboratory equipment, the samples used in the experiment and the experimental procedures are presented, as well as the experimental temperature, pore pressure and moisture migration results.

Chapter 4 presents the thermal and hydraulic numerical models that were developed to predict the thaw consolidation behaviour of the fine-grained permafrost soils tested in the laboratory program. The model layout, material properties, boundary conditions and results are presented.

An analysis of the results is presented in Chapter 5. The laboratory results are analyzed with respect to theoretical predictions from the thaw-consolidation theory and to the numerical modelling predictions.

Finally, conclusions of the thesis and suggested future work are presented in Chapter 6.

## **2 Literature review**

### ***2.1 Thaw consolidation theory***

The thaw consolidation for soil is a complex behaviour due to a combination of mechanical, thermal and hydrological processes. Tsytoich appears to be the first to perform thaw-consolidation tests approximately 70 years ago. In 1937, Tsytoich and Sumgin published a Russian book entitled “Principles of frozen ground mechanics” where they presented the results of thaw-consolidation tests that were performed by Tsytoich (Andersland and Anderson, 1978). The tests were performed using a simple oedometer enhanced with a heated loading cap to measure settlement in rapid thawing soils under different loading conditions. In 1965, Tsytoich performed experimental tests and determined the following two facts (Smith, 1972):

- Pore water pressures in a thawed soil dissipates according to the established Terzaghi consolidation theory;
- Just above the thaw boundary, the pore water pressures remain constant when the rate of thaw is proportional to the square root of time.

Morgenstern and Nixon (1971) presented a thaw consolidation theory. Using the theories of heat conduction and of soil consolidation, equations were formulated to determine the consolidation behaviour of thawing soils, including the excess pore pressures in a thawing soil and a settlement ratio. The complete derivation of the formulated equations can be found in Appendix A.

A one-dimensional configuration was considered in Morgenstern and Nixon’s theory, as shown in Figure 4. The frozen soil is subjected to an increase in temperature at the soil surface, thus the temperature of the frozen ground is lower than the temperature at the surface of the soil.

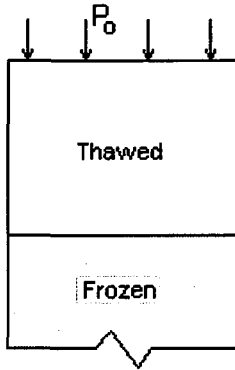


Figure 2.1 One-dimensional thaw consolidation configuration (after Morgenstern and Nixon, 1971)

The position of the thaw front at a certain time during the course of thawing is described by the Neumann solution:

$$X(t) = \alpha\sqrt{t} \quad [2.1]$$

Where  $X$  = depth to the thaw plane  
 $\alpha$  = a thermal constant determined in the solution of the heat conduction problem  
 $t$  = time

Boundary conditions were also defined. Initially, the time is zero and the distance to the thaw plane from the soil surface is zero. Also, the upper surface of the soil mass is assumed to be free-draining, therefore pore water pressures are zero during thawing at the soil surface. Furthermore, if the applied stress does not vary with time, the classical Terzaghi consolidation equation for a saturated compressible soils is given as:

$$c_v \frac{\partial^2 u}{\partial x^2} = \frac{\partial u}{\partial t} \quad [2.2]$$

Where  $c_v$  = coefficient of consolidation  
 $u$  = excess pore pressure  
 $x$  = depth measured from the ground surface

A closed-form analytical solution was assumed with respect to basic soil mechanic equations and the boundary conditions. Using the aforementioned configuration, boundary conditions and theories of heat conduction and of consolidation, the excess pore pressures caused by thawing were derived, resulting in the following expression:

$$u(x,t) = \frac{P_o}{\text{erf}(R) + \frac{e^{-R^2}}{\sqrt{\pi}R}} * \text{erf}\left(\frac{x}{2\sqrt{c_v t}}\right) + \frac{\gamma' x}{1 + \frac{1}{2R^2}} \quad [2.3]$$

Where  $P_o$  = load applied to the surface  
 $R$  = thaw consolidation ratio  
 $\gamma'$  = submerged unit weight of the soil  
 $\text{erf}()$  = error function

The dimensionless thaw consolidation ratio,  $R$ , is calculated with the following equation:

$$R = \frac{\alpha}{2\sqrt{c_v}} \quad [2.4]$$

Furthermore, the following dimensionless variable was introduced:

$$Z = \frac{x}{X(t)} \quad [2.5]$$

Equation [2.3] now becomes

$$u(x,t) = \frac{u(z,t)}{P_o + \gamma' X} = \left(\frac{1}{1+W_r}\right) \frac{\text{erf}(RZ)}{\text{erf}(R) + \frac{e^{-R^2}}{\sqrt{\pi}R}} + \frac{Z}{\left(1 + \frac{1}{2R^2}\right)\left(1 + \frac{1}{W_r}\right)} \quad [2.6]$$

$$\text{Where } W_r = \frac{\gamma' X(t)}{P_0}$$

Morgenstern and Nixon (1971) formulated the two following solutions of excess pore water pressures by reducing Equation 2.6 assuming two extreme loading conditions. Equation 2.7 represents the solution for a weightless material ( $W_r=0$ ) and Equation 2.8 is the solution for a soil consolidating under its own weight ( $W_r=\infty$ ).

$$\frac{u(z,t)}{P_0} = \frac{\text{erf}(RZ)}{\text{erf}(R) + \frac{e^{-R^2}}{\sqrt{\pi}R}} \quad [2.7]$$

$$\frac{u(z,t)}{\gamma' X} = \frac{Z}{\left(1 + \frac{1}{2R^2}\right)} \quad [2.8]$$

From these equations, Morgenstern and Nixon indicated that the excess pore pressures and the degree of consolidation in thawing soils depend primarily on the thaw-consolidation ratio,  $R$ . This parameter is a relation between the rate of thaw and the rate of consolidation of a thawing soil. In their approach, Morgenstern and Nixon found that the excess pore pressure distribution is linear for a given consolidation ratio for the case where the soil is consolidated by the weight of the soil alone. Figure 2.2 shows a plot of the normalized values of excess pore pressures that have been computed for different thaw consolidation ratios. The normalized pore pressures are the excess pore pressures divided by the effective stress.

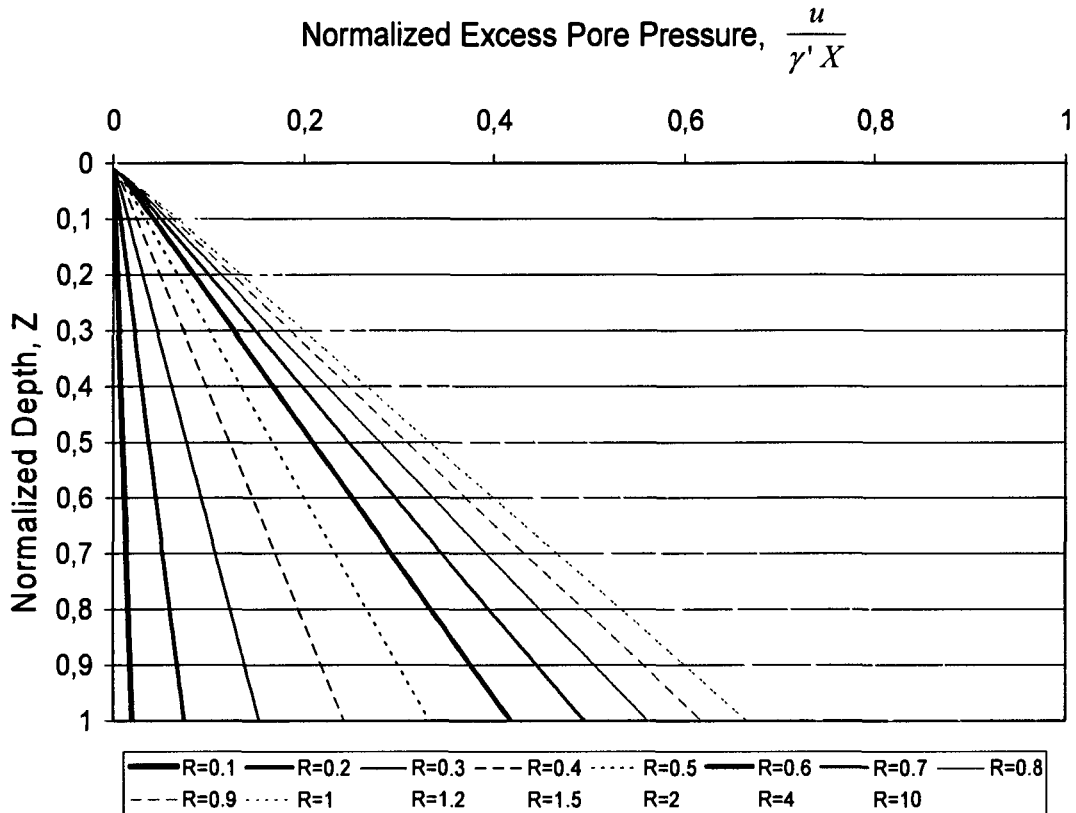


Figure 2.2 Distribution of the normalized excess pore pressures for various thaw consolidation ratios when the soil is consolidated by its own weight

## 2.2 Experimental studies on pore pressure

Since the thaw consolidation theory was developed, many studies have been made relating to pore water pressure. Morgenstern and Smith (1973) examined the results from a special oedometer (Permode) that they designed to assess the validity of the thaw consolidation theory. It was very similar to a standard oedometer; however settlements could be measured to an accuracy of 0.0001 inches as thaw consolidation progressed. The Permode was used to perform controlled thaw-consolidation tests on many remoulded samples of frozen Athabasca Clay, and some on Lake Edmonton Clay and Bentonite, with different index properties (plastic limit, liquid limit, plasticity index, percentage clay and specific gravity). A constant surface temperature was applied to facilitate thawing and pore water pressures were measured at the base of the soil

sample. In agreement with the theory, it was found that the maximum pore pressure at the thaw boundary is a function of the thaw-consolidation ratio for the remoulded clay samples tested. Furthermore, excess pore pressures and settlements in a thawing soil were found to be dependent on the R value, which agrees with the thaw-consolidation theory. Hence the thaw consolidation ratio of soil samples can be determined based on the pore pressure and settlement values measured during the laboratory testing.

Shortly after, Morgenstern and Nixon (1974) presented the results of tests carried out on natural undisturbed samples of fine-grained permafrost. The thaw-consolidation tests were performed using a modified version of the thaw-consolidation apparatus developed by Smith (1972). The samples used for the tests were of frozen cores of sandy silt and of silty clay. Thawing was induced by applying a surface temperature of 26 °C and an overburden load was applied at the surface of the sample. Pore pressures, settlements and temperatures were monitored until thawing and settlement was complete. The excess pore pressures measured at the base of the sample correlated reasonably with the predictions obtained from the Morgenstern and Nixon (1971) theory of thaw-consolidation. Nonetheless, the pore pressures were simply measured at the base of the soil sample.

Following an extensive field study on landslides in the Mackenzie Valley, McRoberts and Morgenstern presented a quantitative analysis of slides at a site on the Mountain River (1974). Their research showed that excess pore pressures play an important role in the shear strength of the thawing slopes (McRoberts and Morgenstern, 1974). McRoberts and Morgenstern (1975) compiled numerous test results to observe pore water during freezing. The result of their study suggests that a coarse-grained sandy soil will expel water while freezing, whereas a fine-grained soil will only expel water when subjected to a higher overburden pressure.

Later, Ryden (1985) tested the validity of the thaw-consolidation theory's predictions for pore pressures in thawing soils. This 1985 study supports the theory that the normalized pore pressures at the thaw front depend upon the value of the thaw consolidation ratio, which is in agreement with the aforementioned study by Morgenstern and Smith. However, the results are valid for an applied loading condition only. Furthermore, the expression that was used to determine the  $\alpha$  value was found to inadequately describe the course of thawing of the soil samples placed in the oedometer.

Eigenbrod et al. (1996) reported results of a unidirectional freezing and thawing test program. Pore pressures and temperature were measured along the perimeter of a fine-grained soil together with water intake and heave. The soil samples consisted of lightly overconsolidated clayey silt of low plasticity. From this study, it was determined that pore-water pressure increases were typically associated with temperature increases following the thawing process. Although, pore water pressures for all measuring points dropped suddenly below 0 kPa as the temperatures first increased above 0 °C, but quickly rebounded back to same value as prior to thaw. Also, maximum positive pore-water pressures were approximately equal to overburden pressure (Eigenbrod et al., 1996).

Since the 1990's, Charles Harris, along with many authors, has done a significant amount of research where pore water pressures were monitored in different types of freezing and thawing tests, on soil samples of different sizes (Harris et al., 1995 (300 mm), Harris and Davies, 1998 (300 mm), Harris et al., 2001 (70 mm), Murton and Harris, 2003 (185 mm), Harris et al., 2003 (70 mm)). The majority of the work cited here refers to a laboratory program simulating periglacial solifluction where soil freezing and thawing takes place. The initial experimental setup was constructed on a 12° slope angle in a refrigerated chamber. In 1995, Harris et al. presented the results of their laboratory simulation of solifluction. The results presented showed that pore pressures

were negative during the freezing process and increased, while generally remaining negative, during the “zero curtain period”. The zero curtain period being referred to as the period of time necessary for the ice to turn in to water, or vice-versa (Muller, 1947). Once the soil had thawed, pore water pressures rose and remained generally positive until the pore pressures had dissipated. However, these positive pore pressures were never in excess of hydrostatic pressure, thus no excess pore pressures were generated.

In 1998, Harris and Davies published a paper presenting the results of their laboratory testing. Pore water pressures were measured during seven cycles of downward freezing and thawing using the same experimental setup as the previously mentioned research. It was noted that positive pore pressures were observed during the freezing stage and negative pore pressures were observed during the “zero curtain period”. Furthermore, excess pore water pressures were generated during the thaw consolidation stage, when downslope displacements were observed.

In 2001, Harris et al. presented the results of similar tests, this time using different slope angles (i.e.  $12^\circ$ ,  $18^\circ$  and  $24^\circ$ ) for centrifuge modelling. Pressure fluctuations that were recorded during the thawing process were found to be equal to those obtained in their previous research. Their results also showed that there was a more rapid drop in pore water pressure on the steeper sloped models. In 2003, these same authors presented results from two centrifuge modelling experiments. Yet again, pore water pressure results were consistent in both experiments. As the sloped soil thawed, the pore pressures increased rapidly to above hydrostatic pressure then slowly decreased as the excess pore pressures dissipated. Also, when comparing the depths of the pressure transducers and the maximum pore pressures recorded by the different transducers during each freeze-thaw cycle, the pore pressures were found to be in part a function of depth, as anticipated.

### **2.3 Summary**

Thaw consolidation theory has been developed in the early 1970's. Some experiments have been conducted to verify the theory and investigate the pore water pressure behavior during thawing of permafrost soils. The experiments have been limited to small samples under loading conditions that are applicable to only part of the thaw consolidation theory. The thaw consolidation behavior for the pore water pressure condition of the permafrost soil under its own weight is a major component of the thaw consolidation theory. However, little study has been done to verify this part of the theory. This thesis is therefore intended to investigate the thaw consolidation and pore water pressure conditions of permafrost soils under its own weight.

### **3 Laboratory Testing**

A laboratory program was setup in order to verify the consolidation behaviour of fine grained permafrost soil for a case where the thawing soil is consolidated by its own weight. This section presents the laboratory apparatus that was developed, a description of the samples that were used for the experiment and the testing procedures.

#### ***3.1 Description of laboratory apparatus***

The laboratory testing was carried out by formulating a device that measures temperature and pore water pressures throughout a fine-grained soil sample while thawing takes place. The device was designed to conduct the freeze-thaw tests in a temperature controlled cold room. The device consists of a soil column surrounded by a silty clay/insulation system, instruments that measure temperature and pore water pressure, and a heating chamber with ventilation system that is placed on top of the soil column and subsequently insulated. A sketch of the device is represented in Figure 3.1.

The permafrost soil sample is contained in a 0.95 meter high pvc cylinder, measuring 15.2 cm in diameter, with the inner surface coated with a Teflon spray to reduce side friction. The cylinder containing the sample is insulated in order to ensure uniform thawing and to reduce heat flow along the sides of the sample. The insulation system was created by placing the cylinder inside two barrels, as shown in Figure 3.2. The first barrel is a Rubbermaid brute container of 55.9 cm in diameter and is filled with silty clay with a high moisture content, similar to the permafrost sample. The cylinder and the first barrel then sit inside a second barrel, which is a 95 gallon salvage drum of 78.7 cm in diameter, and is filled with Thermocell loose-fill insulation. This silty clay/insulation system was designed to minimize lateral boundary effects so that the sample thaws from the top down, which represents natural ground thawing conditions.

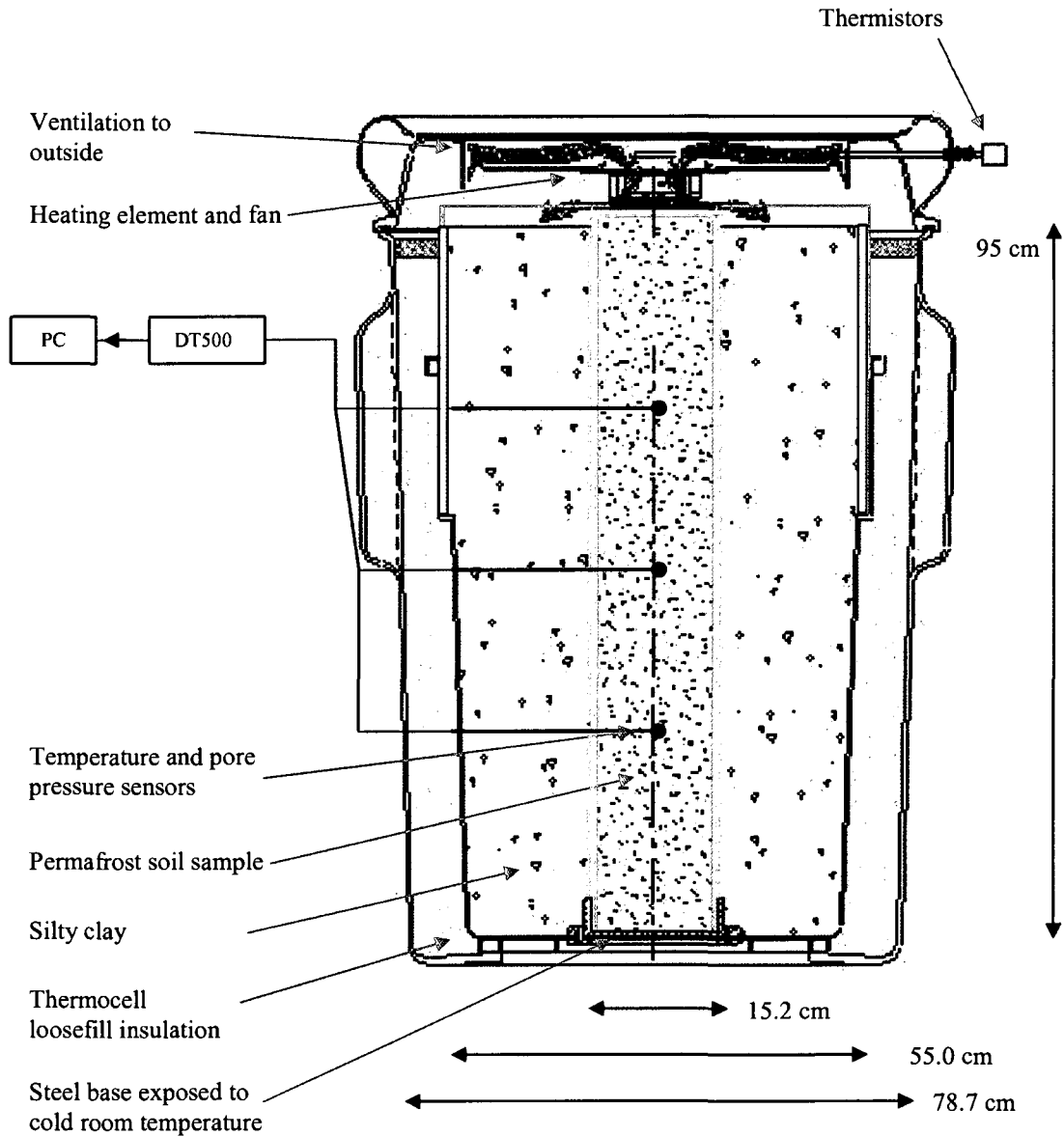


*Figure 3.1 Thaw consolidation laboratory equipment*

The device is placed in a “walk-in” cold room of 3 m in length by 2 m in width. Inside the cold room, the device rests on a stainless steel base plate open to the rooms freezing temperatures to ensure that the boundary conditions at the bottom of the samples are similar to the permafrost conditions, as shown in Figure 3.3.

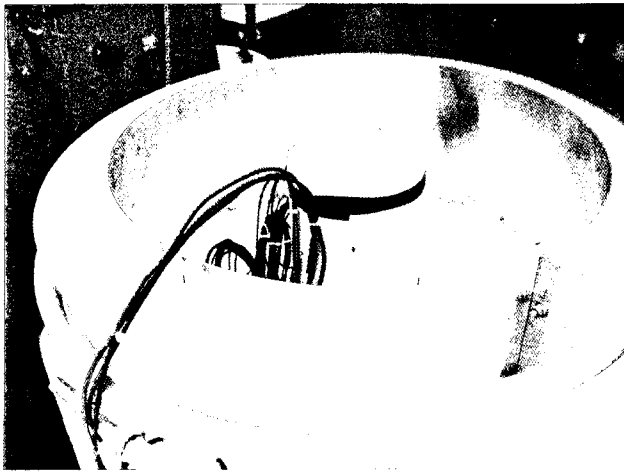


*Figure 3.2 Profile view of the silty clay/insulation system setup*



*Figure 3.3 Steel base of the column open to cold room temperature*

Three holes of 6.35 mm diameter were drilled and tapped along one side of the cylinder at 30, 50 and 70 cm from the top for insertion of the temperature sensors and pore pressure transducers, as shown in Figure 3.4. The temperature sensors are placed at the same depth as the pore pressure sensors in order to keep track of the location of the thaw front when the pressure readings are taken. The cylinder has a total of three K-type thermocouples and three PDCR-81 miniature pore pressure transducers inserted at the specified

depths. The sensors are connected to a DT500 dataTaker data logger. Data were recorded at 10 minute intervals.

The pressure transducers consist of 6.4 mm diameter by 11.4 mm long stainless steel cylinders with porous ceramic filter tips with the ability to measure a maximum pressure of 350 mbar (35 kPa) through a silicon diaphragm, as shown in Figure 3.5. The diaphragm is exposed to the pore water via the porous stone and is connected to a fully active strain gauge bridge for pore pressure measurement. For the purpose of this test, the transducers must be able to withstand freezing and thawing. To ensure this, each the pore pressure measuring system is saturated with an anti-freeze silicone fluid, with a freezing-point of  $-55^{\circ}\text{C}$ , before being inserted into the soils sample.

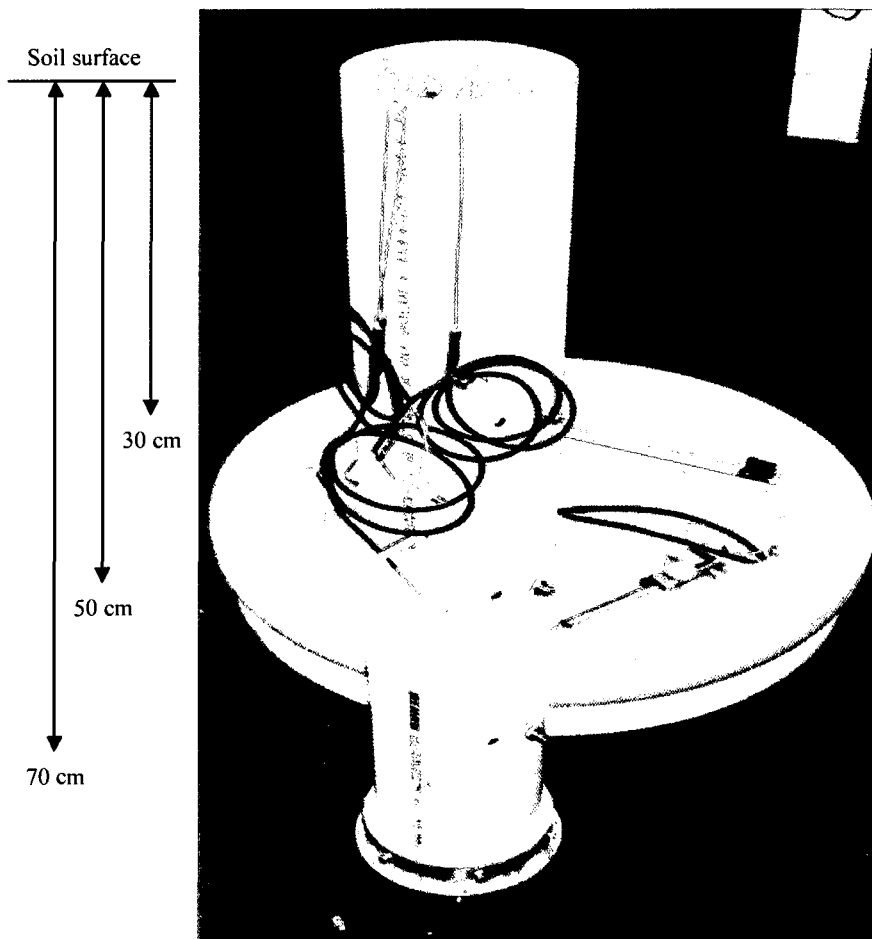


*Figure 3.4 Location of the pressure and temperature sensors*

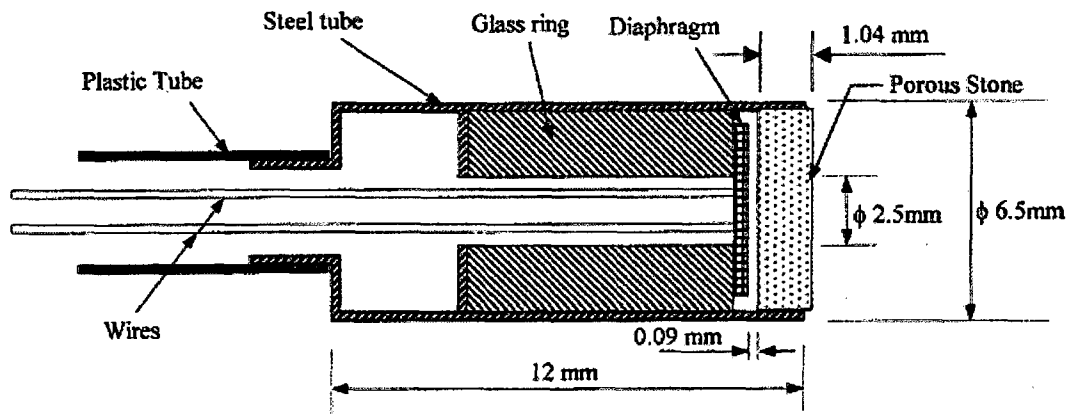
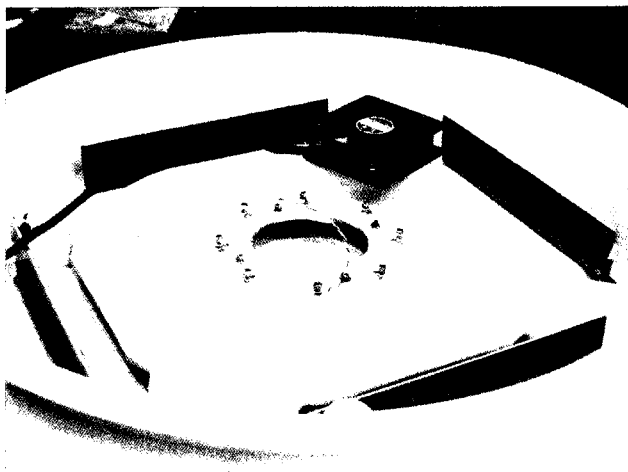


Figure 3.5 Tip of the PDCR-81 miniature pore pressure transducer (after Muraleetharan and Granger, 1999)

A boxed-in heat source is located at the top of the closed system, as shown in Figure 3.1. This heat source consists of 4 silicone rubber enclosure heaters mounted in the lid of the device, as shown in Figure 3.6. These heaters are regulated by two thermistors and connected to a temperature controller that can be manually set to any chosen thawing temperature, and that is located outside the cold room.

A ventilation system was installed to ensure a constant humidity inside the heating chamber. The ventilation system consists of a small fan that is installed inside the heating chamber for air circulation as well as two 12.7 mm clear rubber tubes connecting the heating chamber to outside the cold room (office environment). This set of tubes and fan allows for air circulation within the heating chamber and disposal of any excess humidity. The completed device, ready for freezing and thawing, is presented in Figure 3.7.



*Figure 3.6 Mounting of the 4 silicone heaters in the lid*



*Figure 3.7 Completed thaw-consolidation device*

### 3.2 Description of sample

Unidirectional thawing tests have been carried out on samples of disturbed silty clay from the Mackenzie valley. The soil was obtained by Baolin Wang of Natural Resources Canada, during a geotechnical investigation performed in June 2006, on Gwich'in land near Travaillant Lake, south-east of Inuvik, Northwest Territories. A typical grain size distribution of the soil is shown in Figure 3.8.

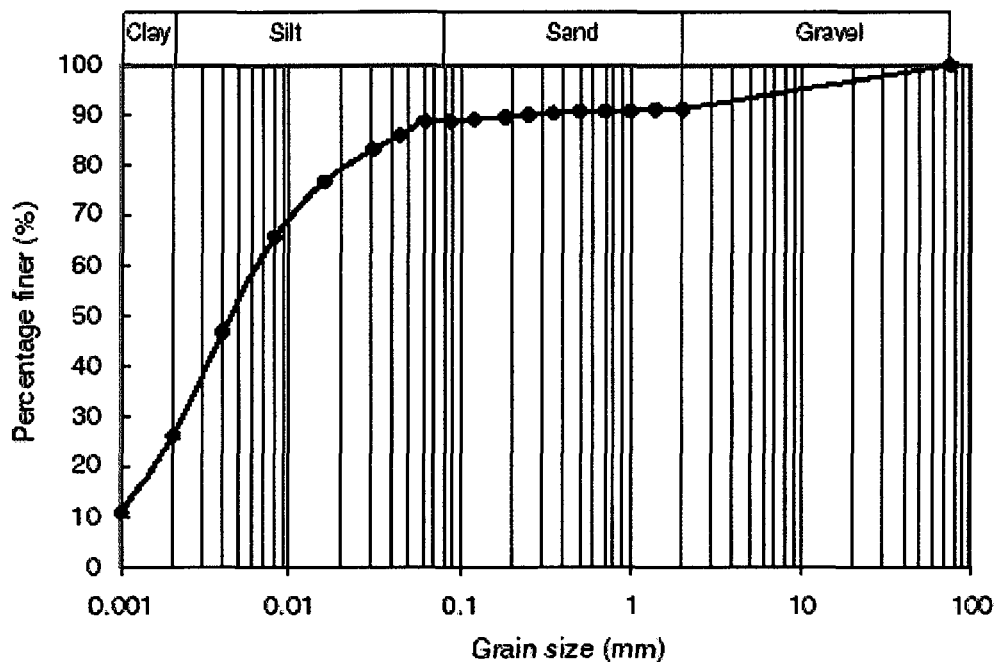


Figure 3.8 Typical grain size distribution (after Su et al., 2006)

The samples used for testing were prepared as to represent the moisture conditions observed at a depth between the active layer and the permafrost observed in the Mackenzie valley. Su et al. (2006) reported that the typical moisture content at such depth is about 40%. The sample was therefore prepared to have a water content of 40%. The prepared sample was allowed to rest for one week in a sealed container in order for the entire sample to attain a uniform water content. After one week, the sample was tested to ensure that it had a uniform moisture content of 40% by weight.

The outer silty clay soil of similar gradation to that of the core sample was obtained from a local source. It is used for minimizing lateral boundary effects, to ensure even downward thawing of the core sample.

### **3.3 Testing Procedure**

Once the sample is prepared with the desired water content, it is carefully poured into the cylinder. Care was taken while pouring the sample into the cylinder to avoid entrapment of air bubbles. Once the slurry has been poured into the cylinder, the pore pressure transducers and temperature sensors are inserted into the designed holes along the cylinder. Again, this will be done carefully to ensure no air bubbles are entrapped in the sample or the sensors. Once the core sample placement is completed, the surrounding barrel is filled with the insulating slurry.

As soon as all soil has been placed, the sample is frozen in the cold room at a temperature of  $-4^{\circ}\text{C}$ , as shown in Figure 3.9. The temperature is monitored throughout the sample by the temperature sensors and the thawing process will begin once the freezing is complete, i.e. when the entire soil column has reached a temperature of  $-4^{\circ}\text{C}$ .

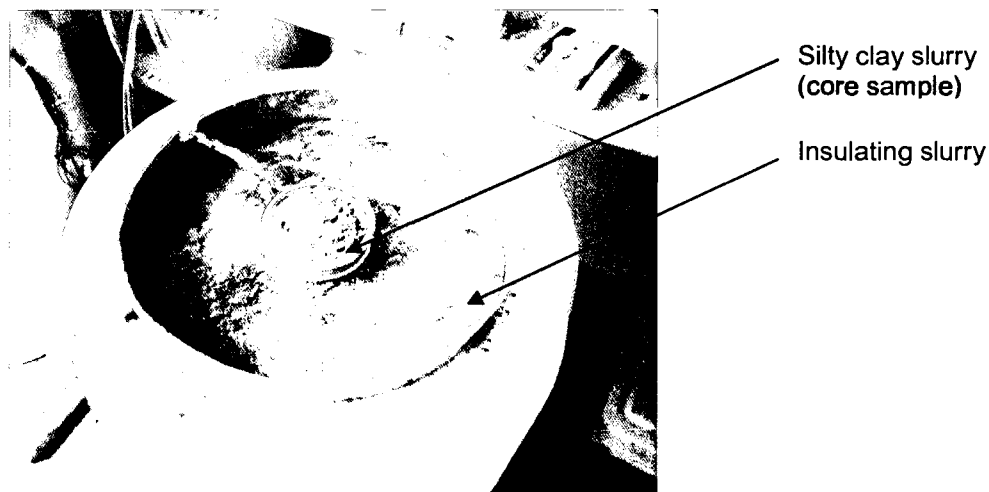


*Figure 3.9 Freezing of fine-grained permafrost samples*

Druck PDCR-81 miniature pore pressure transducers were used to measure the pore water pressures during thaw. Muraleetharan and Granger (1999) evaluated Druck PDCR-81 pore pressure transducers for measuring matric suction in unsaturated soils. Tests were performed on samples of Minco silt to determine the sensitivity of the PDCR-81 to changes in the sensor saturation fluid and moisture contents of the soil samples, as well as the ability of the sensor to produce a soil water characteristic curve and its response to rapid changes in pore water pressures. The test results were also compared with results obtained from a tensiometer and indicated that the PDCR-81 can be used effectively to measure negative pore pressures as well as to quantify matric suction in unsaturated soils. Their results also indicated that transducers saturated in 100% water took less time to reach equilibrium (i.e. 420 seconds), while the transducers saturated in water mixed with 30% glycerine took longer time to reach equilibrium (i.e. 120000 seconds). Thus, the length of time for the transducer to reach and maintain equilibrium proved to be a function of the viscosity of the saturation fluid. This length of time was also found to be a function of the moisture content of the unsaturated soil when the volumetric moisture content in the silty soil samples was gradually increased from 9.4% to 28.0%. As the volumetric moisture content was increased in the soil, the time to reach and maintain equilibrium also increased from 840 seconds to 95000 seconds, respectively. Moreover, results showed that an increase in the pore size of the porous stone will decrease the time for the transducer to reach and maintain equilibrium. Finally, the results suggested that the pore pressure readings will not stay constant after reaching equilibrium, but rather oscillate slightly around the equilibrium value, due to the fact that air is constantly diffusing through the porous stone. In summary, lowering the viscosity in the saturation fluid, using porous stone with higher pore sizes and lowering the moisture contents in the test samples were found to be effective means of increasing the responsiveness of the PDCR-81 pore pressure transducers.

In order to ensure that these sensors would not be damaged during the freezing process, they were saturated with ethylene glycol antifreeze (Harris & Davies, 1998) and calibrated before being inserted in the silty clay soil sample.

Soil specimens are frozen in the designed thaw-consolidation device under closed system conditions (McRoberts and Morgenstern, 1975). Freezing takes place by placing the freeze-thaw laboratory device in a cold room, which was maintained at a temperature of about  $-4^{\circ}\text{C}$ . The top end of the cylinder remains open to the cold room atmosphere. The soil sample freezes from the top down as the sides of the device are insulated to prevent heat flow in the radial direction.

The sample is allowed to freeze for a period of 15 days, or until the temperature sensors indicate that the soil temperatures are below  $-4^{\circ}\text{C}$ . Once the sample is fully frozen, an insulated boxed-in heat source on the top of the sample is turned on to allow thawing to take place. Thawing of the soil sample takes place from the top down. The ventilation system is turned on throughout the thawing test. Thawing temperature is maintained at  $25^{\circ}\text{C}$  in the heating chamber, while the bottom of the soil sample is maintained at the cold room temperature of  $-4^{\circ}\text{C}$ .

Temperature and pore water pressures were monitored at intervals of 10 minutes during the entire freeze-thaw test. Once the testing program was completed, the final soil moisture content was determined at various depths throughout the thawed soil.

### **3.4 Laboratory results**

Three freezing and thawing tests were carried out. Due to some malfunctions with the pore pressure instrumentation, the soil temperature results are presented for all three cases, while pore water pressure results are only presented for the third test.

A heave of 4.2 cm, 3.5 cm and 2.8 cm was observed at the end of the freezing process and a settlement of 9.3 cm, 5.0 cm and 8.4 cm was observed at the end of the thawing process, for sample # 1, sample #2 and sample #3, respectively. The heaving and settlement values were measured using a ruler with respect to the top of the soil column (i.e. 95 cm from the base). The heave measurement being the distance the soil surpassed the top of the soil column following the freezing process and the settlement measurement being the amount the soil settled with respect to the initial 95 cm height, following the thawing process.

### **3.4.1 Temperature**

Figure 3.10 shows the temperature results obtained during the thawing period for two first test samples as well as the cold room temperature during the test. The temperature in the heating chamber was maintained at 25°C and the thawing process was complete after 16 days. At this time, the temperatures in the soil sample had begun to reach equilibrium, as can be seen in Figure 3.10. The cold room temperatures fluctuated every 6 hours. This is due to the slight malfunctions of the cold room temperature controllers. The freezing temperature was therefore set to -6°C rather than -4°C during the first two tests. Furthermore, the oscillating curves on Figure 3.10 depict larger variances during the first 9 days of thaw because it is only after the first 9 days that the high-low controllers were initially adapted for the cold room.

The soil temperature versus time for each sample is presented for the three different depths where the pressure transducers were inserted; 30 cm (light grey curve), 50 cm (dark grey curve) and 70 cm (black curve) from the soil surface, respectively. The solid lines represent the temperature results for sample #1 and the dotted lines are representative of sample #2 (Note: two identical models were built and tested at the same time). Both test samples were prepared at the same time and were subjected to identical freezing and thawing conditions. The

results from the K-type thermocouples that were inserted in both soil specimens indicated that both samples were thawing simultaneously and following the same pattern, which was anticipated as they were similar samples subjected to identical boundary conditions. The results proved that the soil temperature data are reliable.

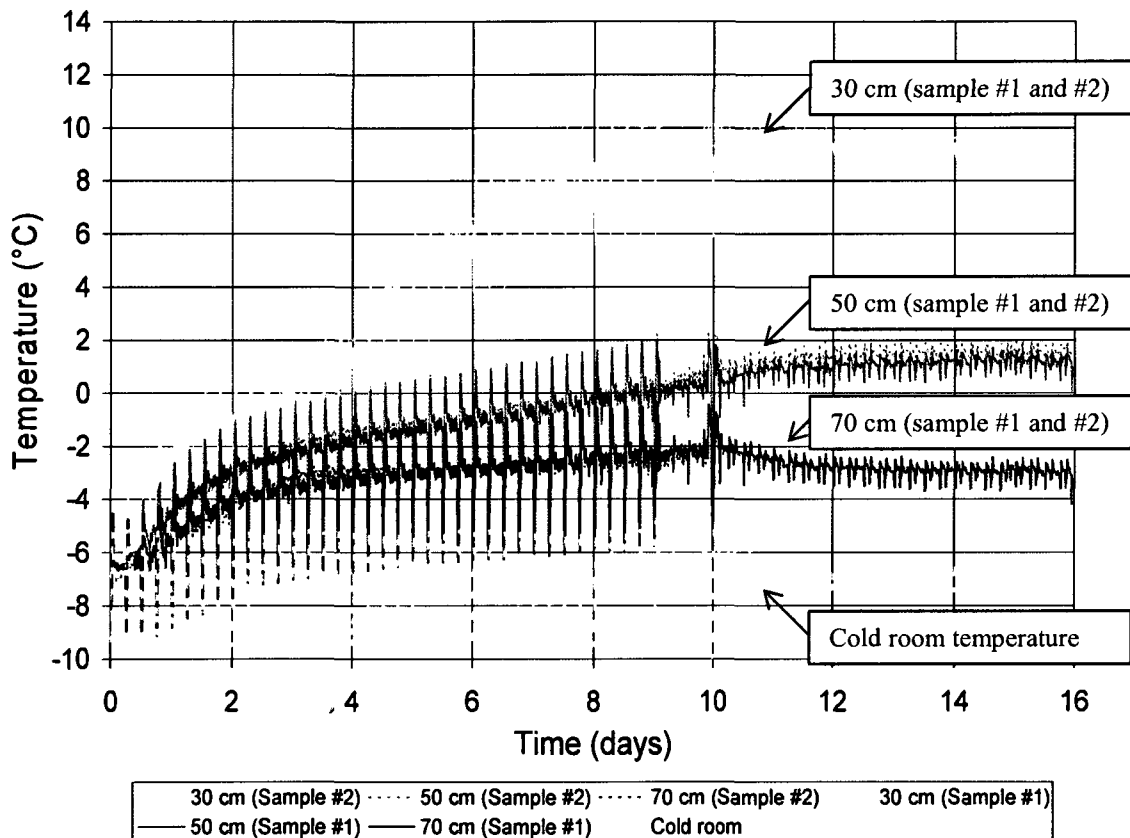


Figure 3.10 Experimental temperature results during thawing of sample #1 and #2

A third thaw-consolidation test was conducted by mixing a new slurry of silty clay, again with a moisture content of 40% by weight. The thawing process for sample #3 was complete after 29 days, which is when the soil temperatures had begun to reach equilibrium. Figure 3.11, shows the cold room and the heating chamber temperature histories during both the freezing and the thawing process for the third test. The initial freezing temperatures show high fluctuations due to

the malfunction of one of the cold room freezing mechanisms. This problem was resolved in the early stages of thawing, i.e. by September 14<sup>th</sup>.

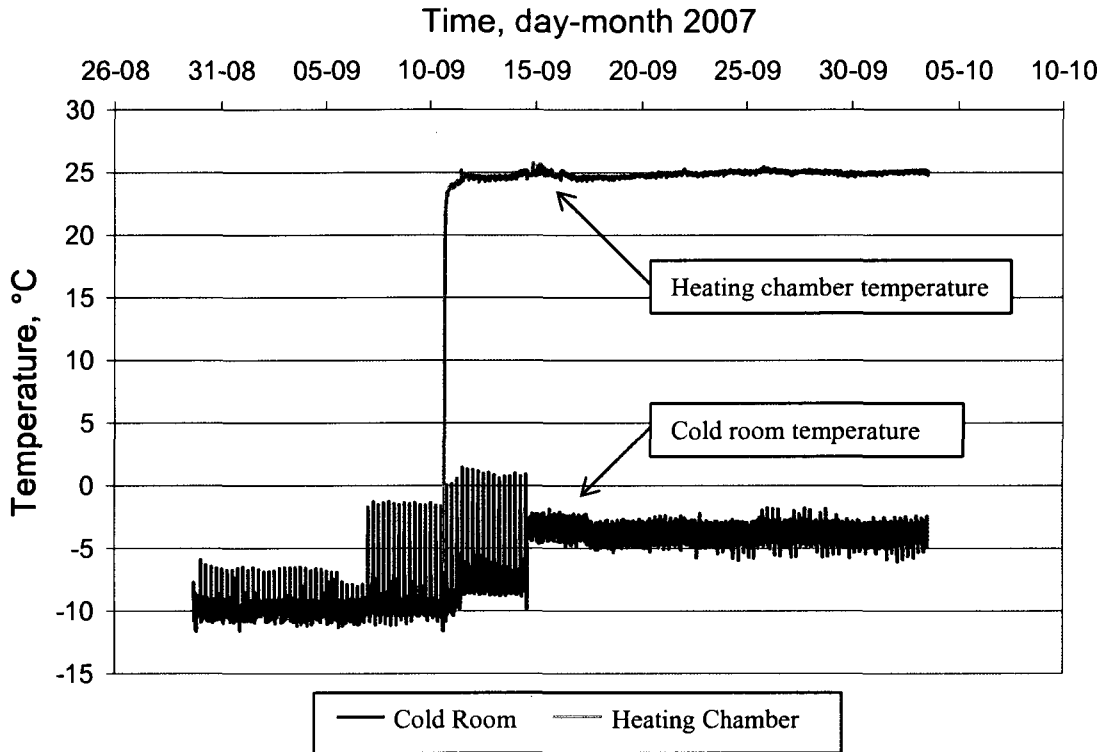


Figure 3.11 Cold room and heating chamber temperatures during freezing and thawing

Figure 3.12 presents the soil temperature results obtained from the thermocouples during the third laboratory analysis at the three different depths where the pressure transducers were inserted. This figure also presents the cold room temperature and the temperature of the heating chamber during the entire thawing process. The cold room temperature was set at -4°C, while the temperature controllers for the heating chamber were set to 25 °C. These boundary temperatures were maintained throughout the test, with the exception of the cold room temperature during the first 3.75 days of freezing, which were set to -7°C. This temperature was slightly lower than the design temperature as there were minor problems with the refrigeration units. One of them was overheating for the reason that warm water was passing through the cooling

pipes. Once this problem was corrected, the temperature in the cold room was set to the desired  $-4^{\circ}\text{C}$ , as shown in Figure 3.12.

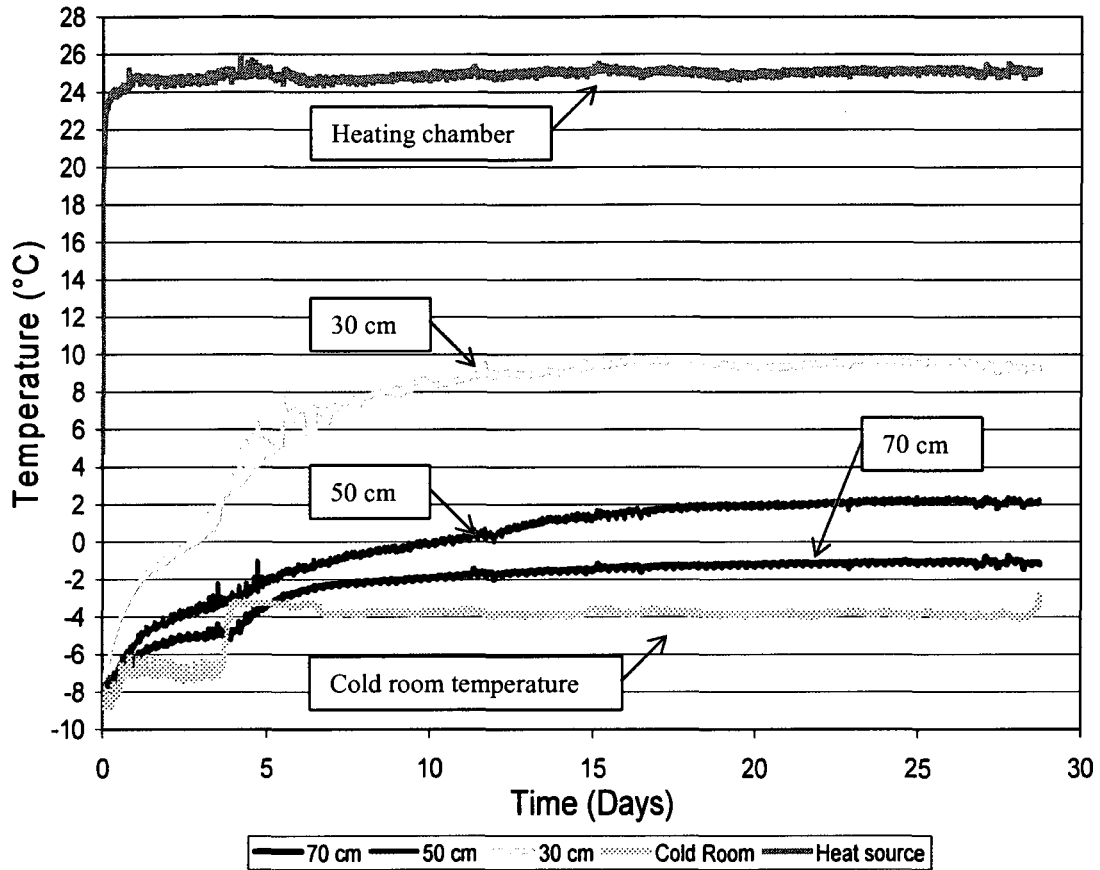


Figure 3.12 Experimental temperature results during thawing of sample #3

### 3.4.2 Pore water pressure

Pore water pressures were monitored during the three laboratory tests with the use of PDCR-81 miniature pore pressure transducers. However, the pore pressure results from the two first test samples are not used for analysis as various instrumental problems were encountered during these tests. This section summarizes the calibration of the pressure sensors for the third experimental trial as well as the pore water pressure results that were obtained from the pore pressure transducers during the third laboratory test.

### 3.4.2.1 Sensor calibration

Some of the pore pressure transducers were damaged during the first two experimental tests. As a result, some minor modifications were brought to the devices before the third test began. Once the PDCR-81 sensors were properly fixed to the data logger, calibration tests were carried out on them. In order to draw a calibration curve for the sensors, they were all placed in three different depths of water and the results were compared with predicted theoretical hydrostatic pressure. The calibration results for three of the six sensors are shown in Figure 3.13 in addition to the theoretical curve.

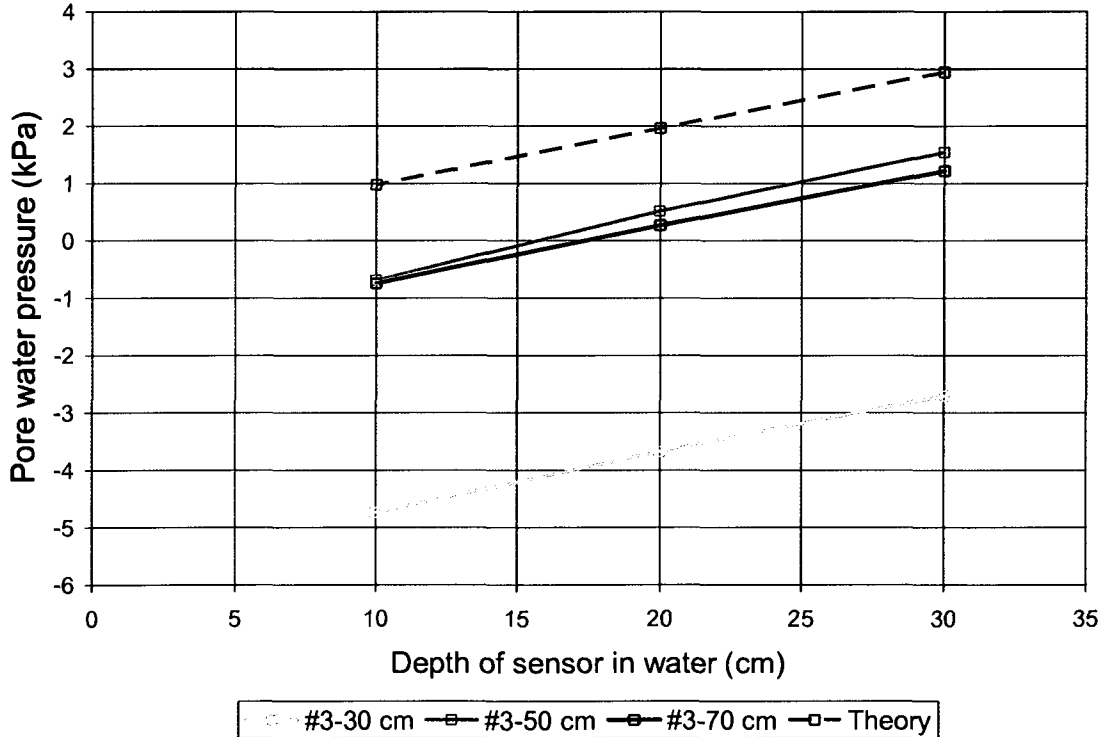


Figure 3.13 Calibration of pore pressure sensors

Figure 3.13 shows that three pressure transducers gave results that followed the same pattern as the theoretical curve, however the results were consistently lower than the actual theoretical values. In order to calibrate the results obtained for the third test, the pressure measurements from sensors #3-30cm,

#3-50 cm and #3-70 cm must to be added to 5.67 kPa, 1.5 kPa and 1.71 kPa, respectively.

### 3.4.2.2 Test data

During thawing, pore water pressures were monitored at 30 cm, 50 cm and 70 cm from the surface of each sample. However, as the soil remained frozen around the sensor located at a depth of 70 cm, only the results from the two higher sensors are presented. Figure 3.14 presents the calibrated pore water pressure results obtained during the thawing period for test sample #3. It is noted from Figure 3.14 that the two pressure sensors registered extreme values when the soil was frozen. Similar behaviour was also reported by Ryden (1985), Eigenbrod et al. (1996), Harris et al. (1995), Harris and Davies (1998) and Murton and Harris (2003). The reason for such response is still yet to be investigated.

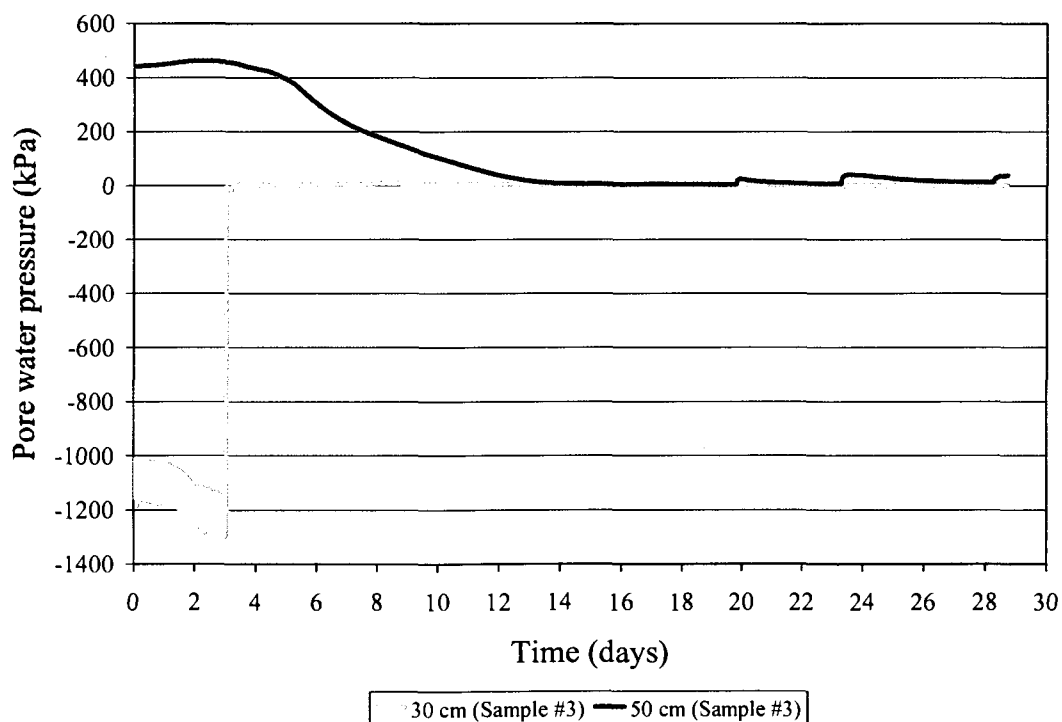


Figure 3.14 Experimental pore water pressure results during thawing of sample #3

In the theory developed by Morgenstern and Nixon (1971), the excess pore pressures in a thawing soil are derived. Figure 3.15 presents the positive excess pore water pressure values that were measured during the thawing of sample #3 within the pressure range of interest. To obtain the excess pore water pressures, the hydrostatic pressures (2.94 kPa for the 30 cm sensor and 4.91 for the 50 cm sensor) are subtracted from the measured calibrated pore water pressure values. These results are further discussed hereinafter.

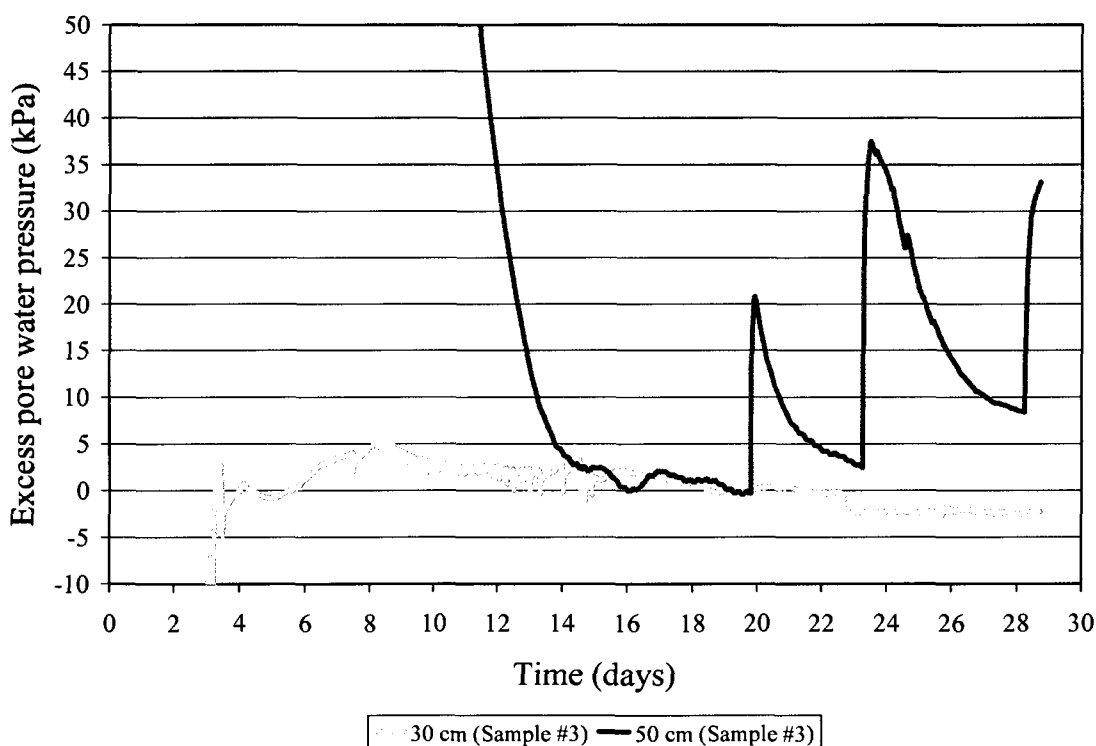


Figure 3.15 Excess pore water pressure results during thawing of sample #3

### 3.4.3 Soil moisture change

Moisture contents of the soil samples were measured at various depths both previous to and following the thaw consolidation tests. When the column was initially filled with the test material, before the freezing process, two specimens

from each device were collected for moisture content measurement. Results indicated that the gravimetric water content in each sample was 41.7%, 38.0% and 40% for devices #1, #2 and #3, respectively. Therefore, all samples had a water content within the desired water content range observed in the field (i.e. 40%). Once the thaw-consolidation tests were complete, the soil was removed from the columns and specimens were taken at various depths for laboratory measurement of moisture content.

Figure 3.16 presents the moisture content, by weight, measured within the silty clay soil in sample #1 and sample #2 after 16 days of thawing, as well as the moisture content measured in sample #3 after 29 days of thawing.

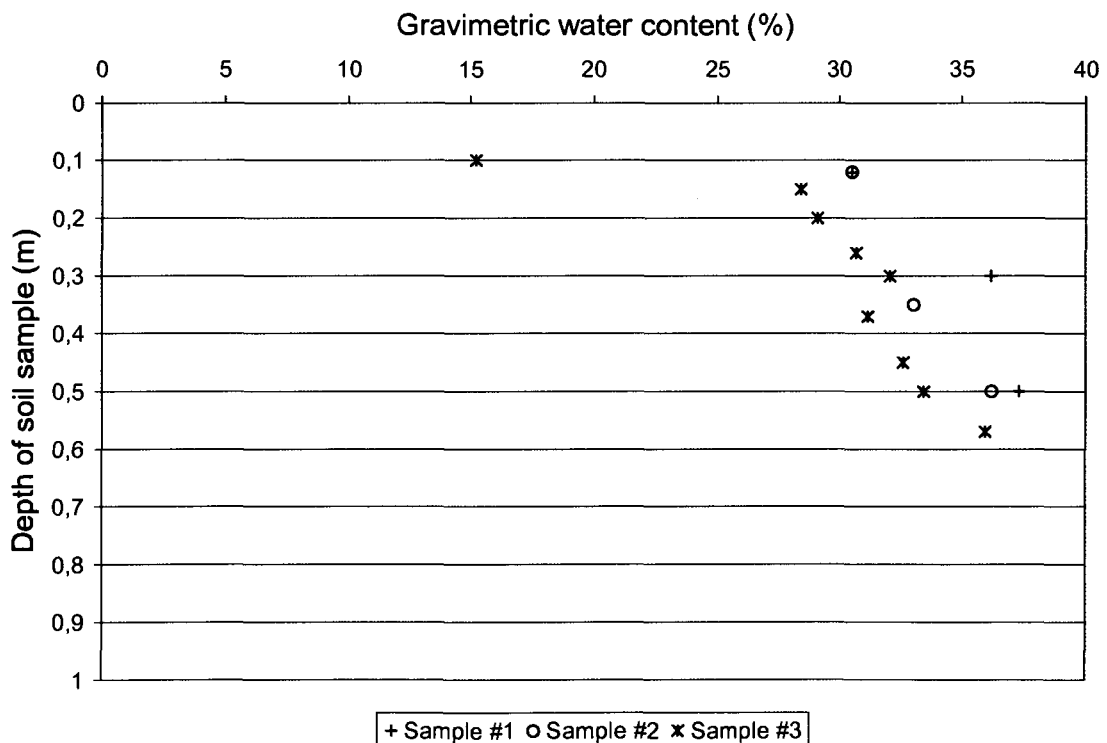


Figure 3.16 Gravimetric water content for samples #1, #2 and #3 at different depths, following the thawing process

## **4 Numerical modelling**

Numerical models were developed in order to assess the effectiveness of the laboratory model to simulate natural thawing conditions. The modelling was carried out using two different finite element software packages, specifically Temp/W and Vadose/W, developed by Geo-Slope International (2007), to respectively verify the thermal and hydraulic behaviour of the thawing soil specimens during the laboratory procedure.

### ***4.1 Thermal modelling using Temp/W***

For the thermal analysis, Temp/W software was used. Temp/W is a two-dimensional finite element software that simulates ground thermal behaviour response to boundary condition changes. The software can be applied to a wide variety of geothermal problems such as the degradation of permafrost, frost depth penetration, effectiveness of various insulation alternatives for reducing freezing and/or thawing, and many more. Temp/W is designed to account for absorption or release of latent heat through freezing and thawing of water and ice, respectively, by means of an unfrozen water content function. Furthermore, once the model has been set up and solved, the software is designed to generate plots of various computed parameters, such as temperature, flux, evaporation, latent heat, etc. (Geo-Slope International Ltd., 2007a).

#### ***4.1.1 Model descriptions and boundary conditions***

The two-dimensional Temp/W model constructed for the thermal analysis is shown in Figure 4.1. The dimensions of the model were defined as to simulate the silty clay soil subjected to thawing during the laboratory test. This model has a height of 0.95 m and a width of 0.55 m. It should be noted that the numerical model is a two-dimensional case, while the laboratory model is actually a three-

dimensional case. However, the extreme boundary conditions discussed in the analysis takes the difference into account.

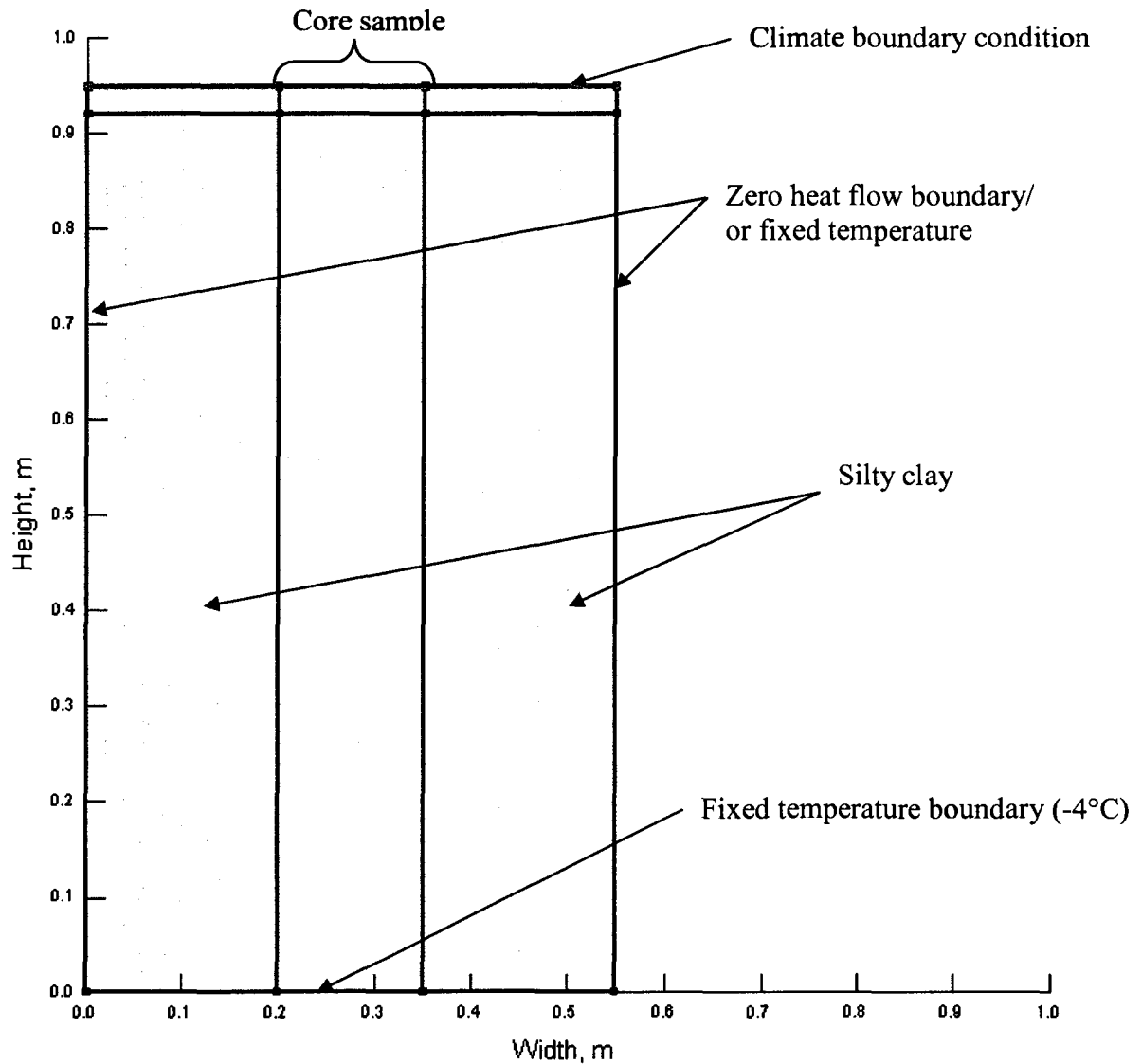


*Figure 4.1 Finite element mesh constructed for thermal analysis*

The thermal analysis was conducted in two stages. First, a steady-state model was setup in order to set initial conditions for the transient model. The entire steady-state model was assumed to have an initial and constant temperature of  $-7^{\circ}\text{C}$  throughout the entire mesh, which represents the temperature conditions setup during the freezing stage and right before the start of the thawing stage of

the laboratory procedures. Also, it was assumed that no heat was flowing in or out of the model's lateral boundaries (total nodal flux,  $Q = 0$ ). Next, a transient model was setup using the steady state model results for the initial conditions. A climate boundary condition was applied at the surface of the model. The climate data used in the analysis is presented in Table 4.1 and is constant throughout the analysis. The temperature of 25°C represents the applied temperature from the heating chamber at the top of the soil sample during the laboratory testing. The relative humidity is an average value assumed based on the fact that it does not largely affect the results analysis, which is driven by the temperature. The wind speed of 3 m/s represents the actual speed of the fan located in the heating chamber, determined from the manufacturer. Finally, pan evaporation was measured in the laboratory by placing two beakers of water under the heating chamber, at the top of the soil column, and allowing the water to evaporate for 24 hours under the same conditions as imposed during the thaw consolidation tests. It was measured that an average of 8 mm of water can potentially evaporate in one day under the imposed laboratory thawing conditions.

*Table 4.1 Climate data applied as surface boundary condition*

Temperature (°C)	Relative Humidity (%)	Wind	Precipitation	Potential evaporation
		(m/s)	(mm)	(mm/day)
25	50	3	0	8

The climate boundary condition was applied at the surface of the transient model and a fixed temperature of -4°C was applied on the bottom boundary of the model. As for the lateral sides of the model, two extreme cases were assumed, given that there was Thermocell loose-fill insulation surrounding the soil sample, but the effectiveness of the insulation was not known. For the first case, it was assumed that there was no insulation on the sides of the model. A temperature

of  $-4^{\circ}\text{C}$  was applied on both lateral sides, which represented the cold room temperature during thawing. For the second case, it was assumed that the sides of the model were fully insulated (i.e. no heat flow in or out of the sample), which represents an ideal situation.

#### **4.1.2 Material properties**

Atterburg Limit tests were performed on the silty clay permafrost collected during the field investigations. The samples tested were found to have a liquid limit, plastic limit and plasticity index of approximately 64%, 28% and 36%, respectively. The atterburg limits results are summarized in Table 4.2.

*Table 4.2 Atterburg limits*

Liquid Limit (Wl)	64.3
Plastic Limit (Wp)	27.6
Natural Water Content (Wn)	23.7

Laboratory testing was carried out to determine soil parameters required for the numerical and theoretical solutions. These parameters are listed in Table 4.3.

*Table 4.3 Soil parameters determined before the freezing process*

Dry unit weight, $\gamma_d$ ( $\text{kN/m}^3$ )	13.03
Unit weight, $\gamma$ ( $\text{kN/m}^3$ )	18.24
Initial gravimetric water content, w (%)	40
Void Ratio, e	1.03

These parameters are assumed reasonable when compared to soil properties found in the literature. Das (2004) presents typical values of dry unit weight, saturated moisture contents by weight and void ratio for soft clays. These values range from 11.5 to 14.5  $\text{kN/m}^3$ , 30% to 50% and 0.9 to 1.4, respectively.

The values determined in the laboratory are within the typical range presented by Das (2004), therefore reasonable for this investigation.

Further parameters were required for the analysis, however not measured in the laboratory. These parameters were assumed from the literature and are outlined in Table 4.4.

*Table 4.4 Silty clay soil parameters determined from the literature*

Parameter	Value used for analysis	Reference
Specific gravity, $G_s$	2.7	Das (2004)
Hydraulic conductivity, $k$ (cm/s)	$10^{-5}$ (silt) - $10^{-7}$ (clay)	Das (2004)
Coefficient of volume compressibility, $m_v$ ( $m^2/kN$ )	$1 \times 10^{-5}$	Krahn (2007)
Coefficient of consolidation, $c_v$ ( $cm^2/s$ )	$1.4 \times 10^{-3}$ - $1.6 \times 10^{-4}$	U.S. Department of Navy (1971), Terzaghi et al. (1996)

Table 4.4 presents a range for the coefficient of consolidation ( $c_v$ ) of the silty clay sample. As this parameter was not measured in the laboratory, a first estimate was made from the coefficient of consolidation chart presented by the U.S. Department of the Navy (1971) for silts and clays. This chart is presented in Figure 4.2. As we have a disturbed soil sample, the value of  $c_v$  should lie below the lower curve. The liquid limit determined in the laboratory was 64.3. This would indicate that a reasonable estimate of  $c_v$  would be  $2.4 \times 10^{-4} cm^2/s$  for the silty clay soil sample, according to the chart.

Figure 4.3 presents a comparison of values of coefficient of consolidation for various clays, computed from two different equations (Terzaghi et al., 1996). It is observed from Figure 4.2 and Figure 4.3 that  $c_v$  generally decreases with an increasing liquid limit. However, Figure 4.3 provides evidence that  $c_v$  may significantly vary for clays with a particular liquid limit. For a liquid limit of 65%,  $c_v$  varies from  $1.59 \times 10^{-4} cm^2/s$  to  $2.5 \times 10^{-3} cm^2/s$ . Thus, with a combination of

Figure 4.2, Figure 4.3 and the known liquid limit of the silty clay soil sample tested in the laboratory, it is reasonable to assume that the coefficient of consolidation of the sample lies within the range of  $1.6 \times 10^{-4} \text{ cm}^2/\text{s}$  (i.e. minimum value from Figure 4.3) to  $1.4 \times 10^{-3} \text{ cm}^2/\text{s}$  (i.e. maximum value from Figure 4.2).

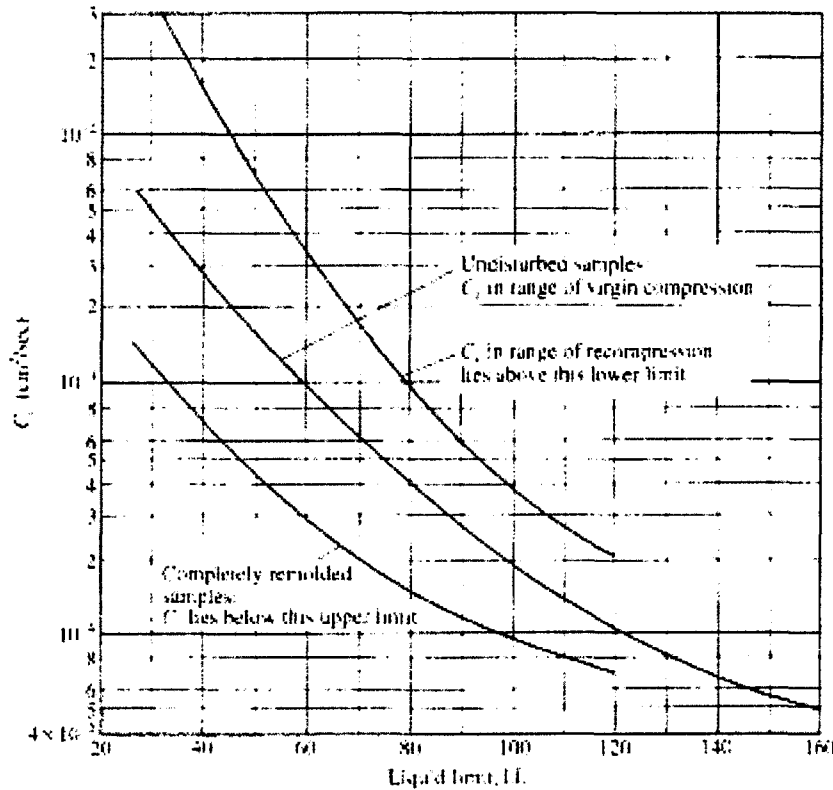


Figure 4.2 Range of coefficient of consolidation for silts and clays (after U.S. Department of the Navy, 1971)

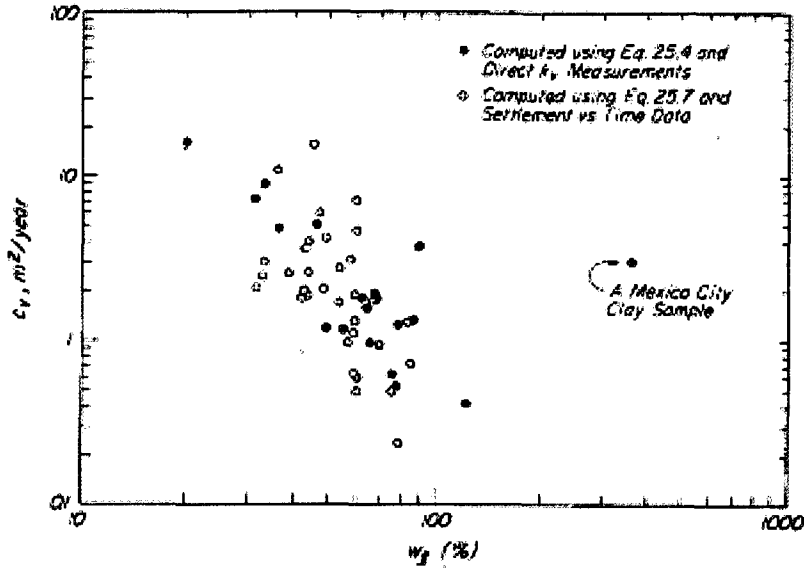


Figure 4.3 Comparison of the computed coefficient of consolidation for various clays (after Terzaghi et al., 1996)

Table 4.5 outlines the volumetric heat capacity (frozen and unfrozen) and water content used for the analysis. The thermal conductivity and unfrozen water content functions used in the analysis are presented in Figures 4.4 and 4.5. These parameters were estimated based on various sources: McRoberts and Morgenstern (1974), Krahn (2004), Kersten (1948), Isaacs (1974), Goodrich (1982), Penner (1970), Smith and Riseborough (1985) Tarnawski (1993) and Zoltai and Pettapiece (1973).

Table 4.5 Volumetric heat capacity and water content

Volumetric heat capacity, C (kJ/m <sup>3</sup> /°C)		Volumetric water content, $\theta$
Frozen	Unfrozen	
2050	2450	0.52

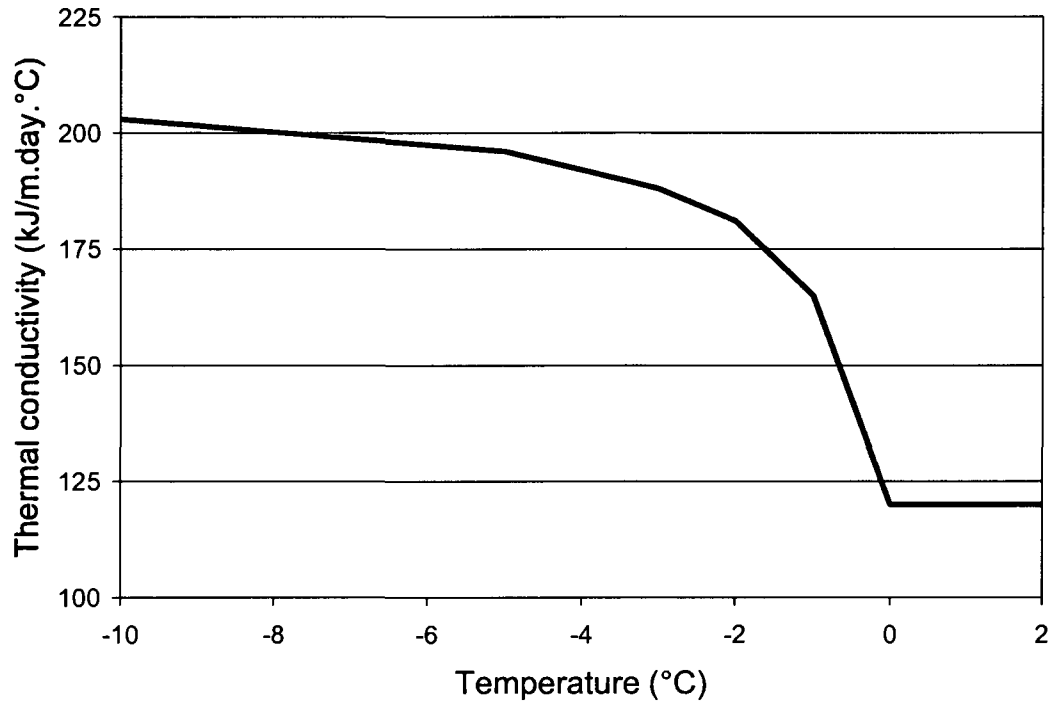


Figure 4.4 Thermal conductivity function used in the analysis

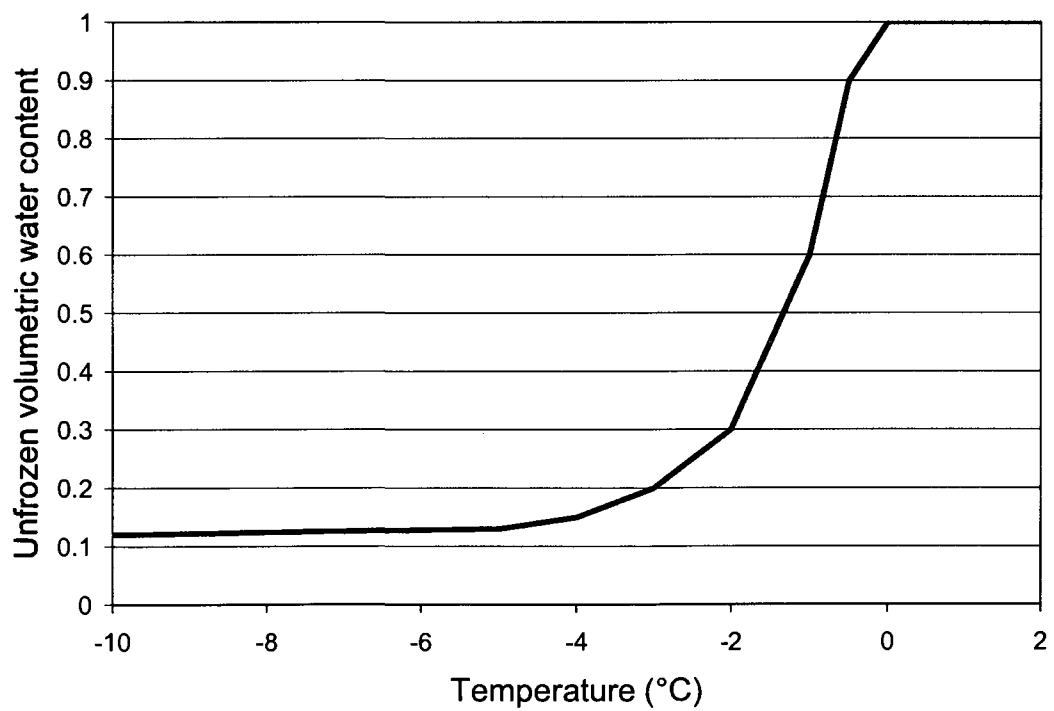
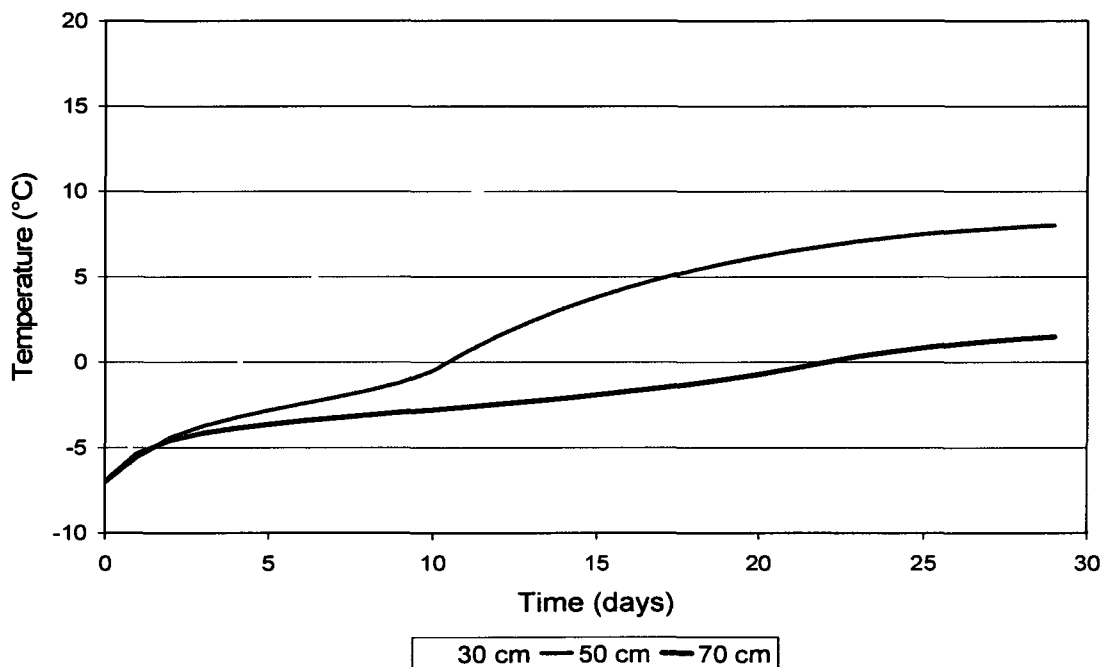


Figure 4.5 Unfrozen volumetric water content function used in the analysis

### 4.1.3 Results

The numerical models developed for both thawing scenarios (i.e. no insulation and fully insulated) were solved for a total of 29 days. The thawing temperatures results versus time, during the entire length of thawing, are presented in the two following figures. Figure 4.6 presents the temperature results for soil located at 30 cm, 50 cm and 70 cm from the soil surface, for a case where the soil would be fully insulated. Figure 4.7 presents the temperature results versus time for a case where the soil would not be insulated. The results are further discussed later.



*Figure 4.6 Soil temperatures with time predicted by the Temp/W model for the case where the soil is fully insulated along lateral boundaries*

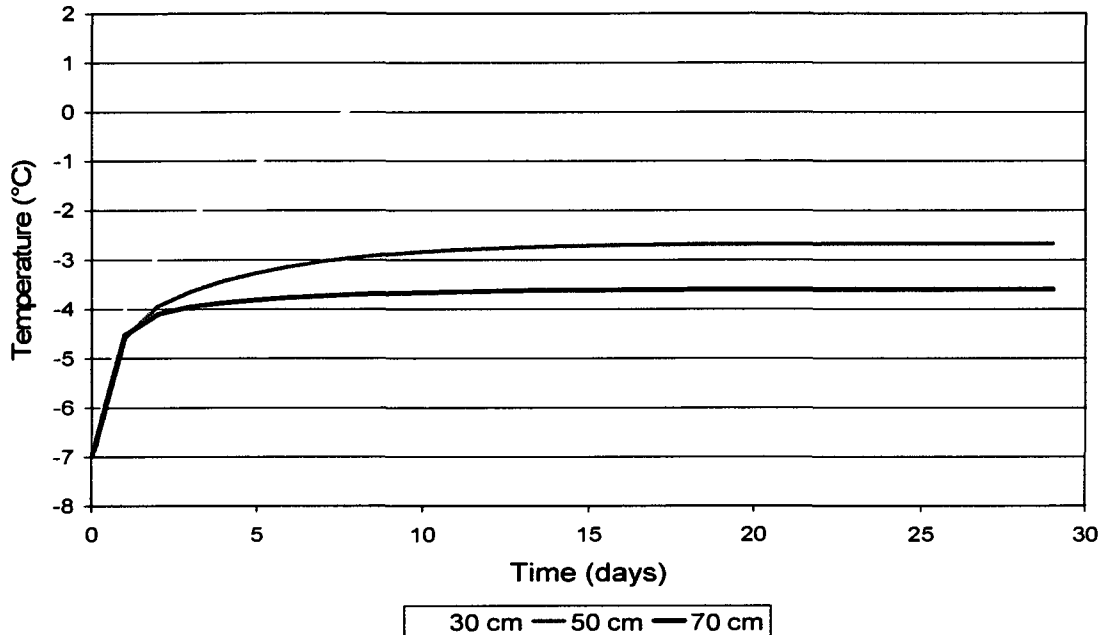


*Figure 4.7 Soil temperatures with time predicted by the Temp/W model for the case where the soil is not insulated along lateral boundaries*

## **4.2 Moisture modelling using Vadose/W**

Vadose/W software was used to predict the hydraulic behaviour of the soil during the laboratory experiment. Vadose/W is a two-dimensional finite element software that simulates flow of water through both saturated and unsaturated soils. Using Vadose/W, two-dimensional water flow can be analyzed by establishing boundary conditions and pore water pressure conditions, such as precipitation, evaporation/transpiration, vegetation, gas diffusion, etc (Geo-Slope International Ltd., 2007b). However, it is not capable of modelling excess pore water pressures generated from thawing of pore ice. The model was used to have an approximate estimate of moisture changes within the thawed zone. The information will provide insight into understanding how the laboratory model performed.

### **4.2.1 Model descriptions and boundary conditions**

The model constructed for the Vadose/W analysis is shown in Figure 4.8. The height of the model is 95 cm, which is the height of the soil column developed for the laboratory analysis. It should be noted that this is actually a one-dimensional case simulated with a two-dimensional model. This is considered reasonable as the laboratory test to be simulated is not expected to have lateral water flow.

Hydraulic, thermal and climate boundary conditions were set for the analysis. The model was developed in two stages for the hydraulic analysis. The first stage was a steady-state setup in order to determine the initial conditions of the model. The boundary conditions for the steady-state model were configured so that it results in a uniform volumetric water content of 0.52 (i.e, 40% by weight) throughout the model for input to the next stage analysis.

For the second stage of the model, the results of the previous setup were used for the initial conditions. A thermal boundary condition of  $-4^{\circ}\text{C}$  was applied at the bottom boundary of the model and the climate boundary condition presented in Table 4.1 was applied at the top surface of the model. Finally, no water was flowing in or out of the lateral boundaries.

Once the boundary conditions were set, the transient model was analyzed for the amount of days corresponding to the thawing period observed in the laboratory.

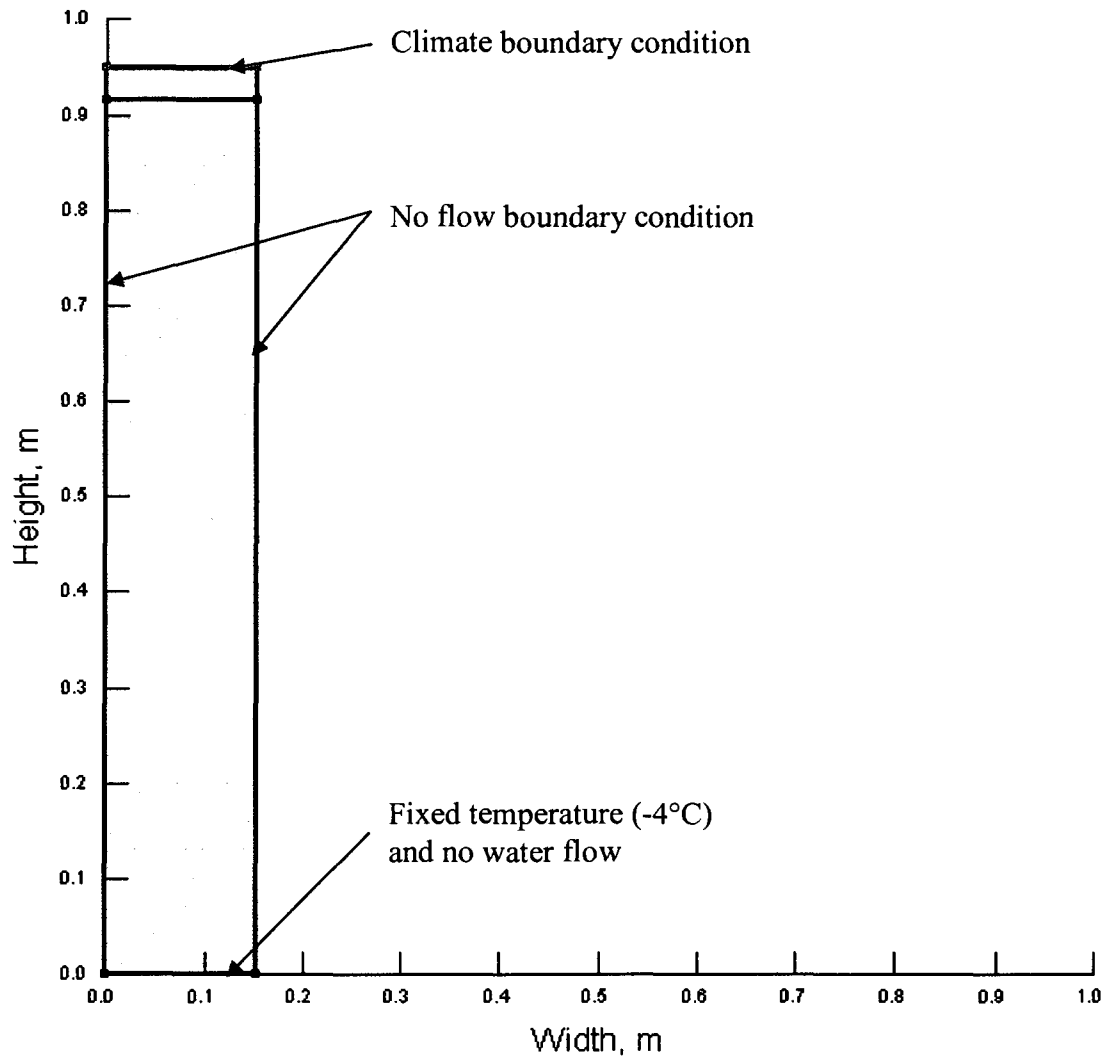


Figure 4.8 Finite element mesh constructed for Vadose/W analysis

#### 4.2.2 Material properties

Table 4.6 outlines the soil thermal properties entered for the analysis. The thermal properties were determined from the same sources as listed for the Temp/W model. Hydraulic properties were established for the Vadose/W model and the functions used for the software solutions are presented in Figure 4.9 and 4.10.

Table 4.6 Material properties used for the Vadose/W analysis

Thermal Conductivity (kJ/day/m/°C)		Volumetric heat Capacity (kJ/m <sup>3</sup> /°C)	
Frozen	Unfrozen	Frozen	Unfrozen
200	120	2050	2450

The soil water content function, or soil water characteristic curve (SWCC), is an important function that presents the capability of the soil to store water under various matric pressures (i.e, pore water pressures). This function is mainly influenced by soil particle size and distribution. A SWCC estimation method provided with Vadose/W was used for estimating the volumetric water content function. With this method, typical water content functions are provided for different soil types. A silty clay soil was selected from the Vadose/W database and a saturated volumetric water content of 0.52 (i.e, 40% by weight) was specified. The soil water content function estimated by Vadose/W is presented in Figure 4.9.

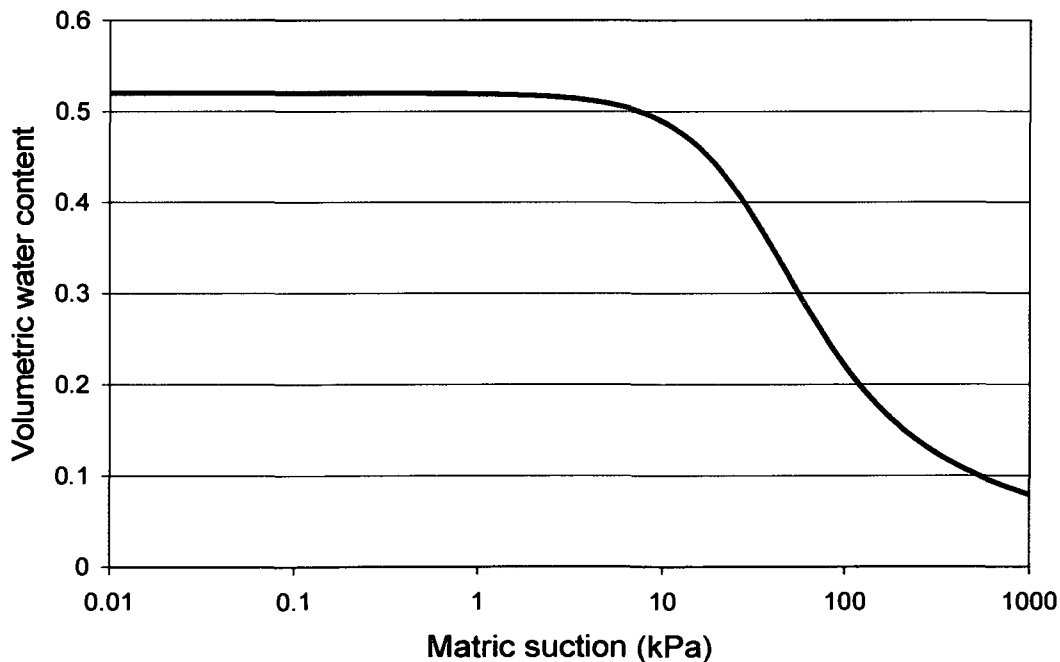


Figure 4.9 Volumetric water content function for silty clay

Another soil material property that is required in the solution of the Vadose/W partial differential equations is the hydraulic conductivity function. The hydraulic conductivity function was estimated using the Fredlund and Xing (1994) method provided with the Vadose/W software. This method estimates the hydraulic conductivity function by using a specified volumetric water content function and a specified value of hydraulic conductivity for the saturated condition.

The volumetric water content function used for the Fredlund and Xing method was the one predicted from the sample functions estimation method, as presented in Figure 4.9. The hydraulic conductivity used for this method was assumed from the literature. As previously presented in Table 4.4, an upper bound and a lower bound hydraulic conductivity was used for the analysis (i.e.  $10^{-5}$  cm/s and  $10^{-7}$  cm/s), therefore two hydraulic conductivity functions were established. The hydraulic conductivity function estimated by the Fredlund and Xing method is presented in Figure 4.10.

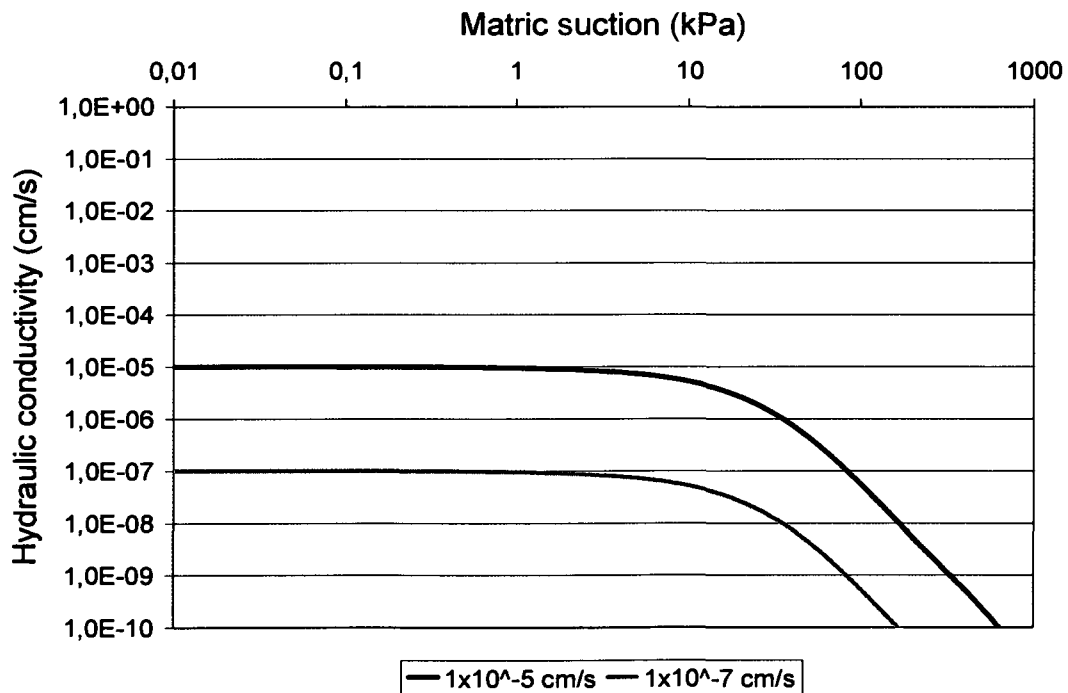


Figure 4.10 Hydraulic conductivity function for silty clay

### 4.2.3 Results

One model was developed for each extreme value of hydraulic conductivity and solved for a total of 29 days. The change in volumetric water content results versus time are presented in the two following figures. Figure 4.11 presents the change in moisture content results with time, at depths of 30 cm, 50 cm and 70 cm from the soil surface, for a soil having a saturated hydraulic conductivity of  $10^{-5}$  cm/s. Figure 4.12 presents the change in moisture content results versus time for a soil having a saturated hydraulic conductivity of  $10^{-7}$  cm/s. The results are discussed hereinafter.

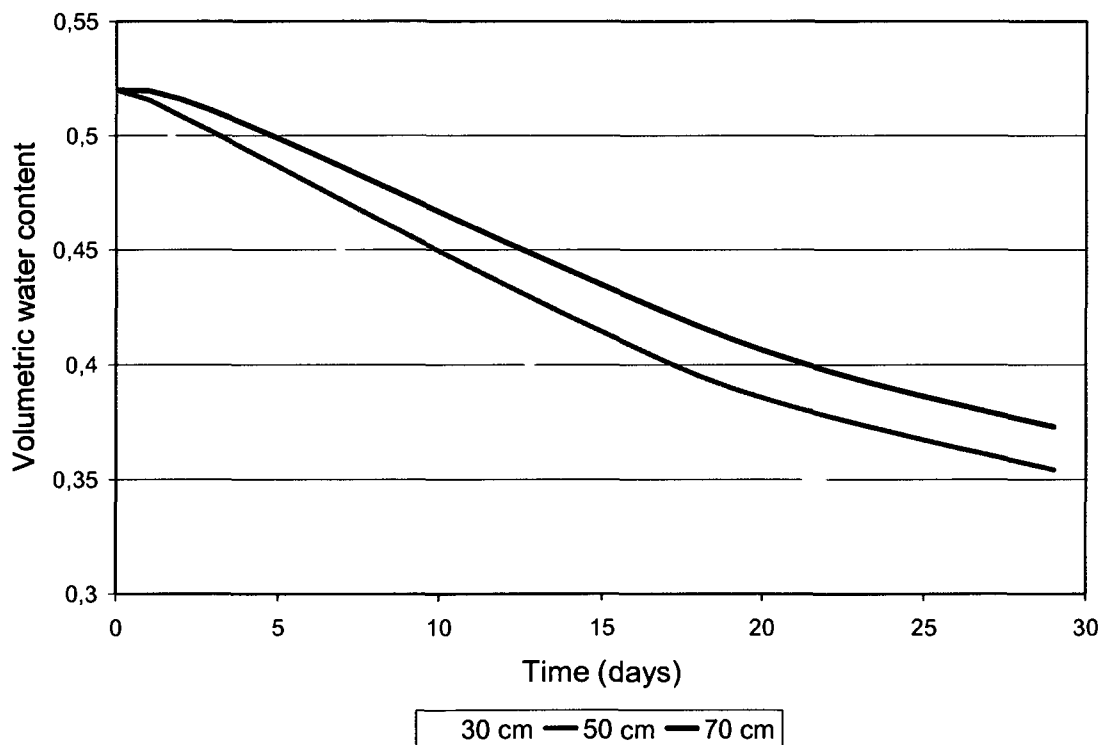


Figure 4.11 Volumetric water content with time predicted by the Vadose/W model based on a saturated hydraulic conductivity of  $10^{-5}$  cm/s

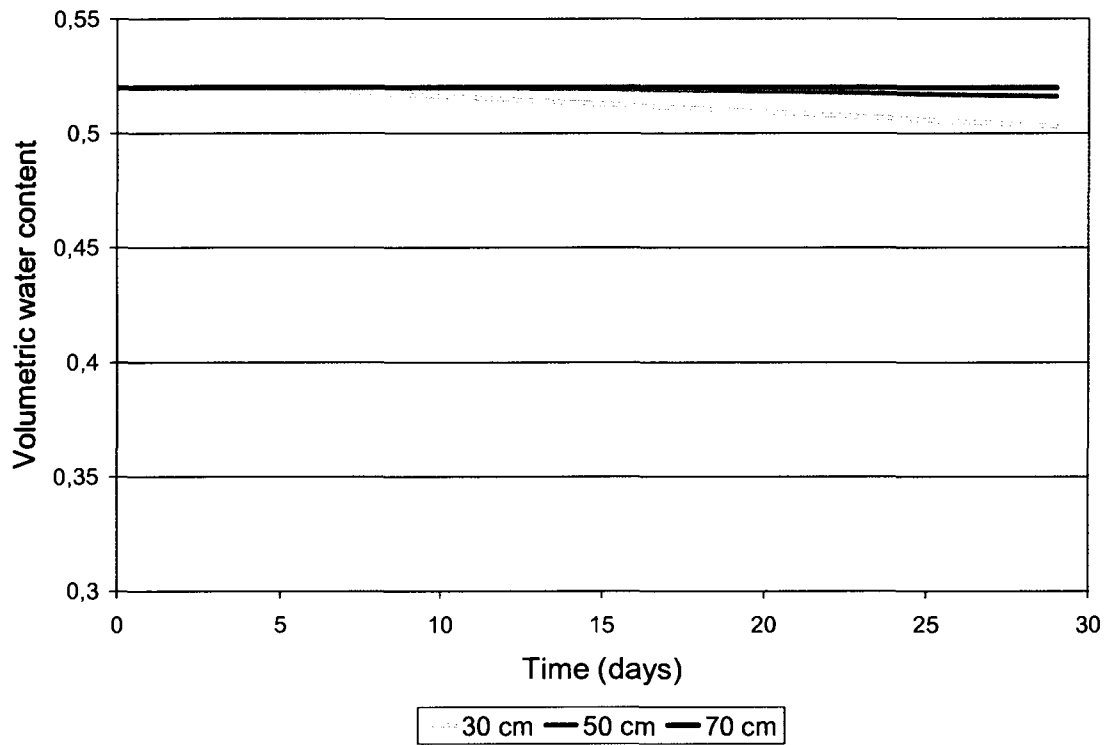


Figure 4.12 Volumetric water content with time predicted by the Vadose/W model based on a saturated hydraulic conductivity of  $10^{-7}$  cm/s

## 5 Analysis

This section provides an analysis of the laboratory results with respect to numerical and theoretical predictions.

It should be noted that, to date, no numerical models can precisely represent the highly complex and highly coupled mechanical-thermal-hydraulic processes occurring in a soil matrix during thaw consolidation, as presented in Figure 5.1. Through coupled processes, many parameters are changing with time and/or with depth, such as volume, void ratio, stress, hydraulic conductivity, water content, suction, temperature, thermal conductivity, specific heat, evaporation, etc. Due to the limitations of the software used, it was not in the interest of this study to compare the numerical predictions to the theory developed by Moregenstern and Nixon (1971). Furthermore, due to time constraints and its complex nature, not all of the coupled processes occurring during thaw consolidation were analyzed during this study.

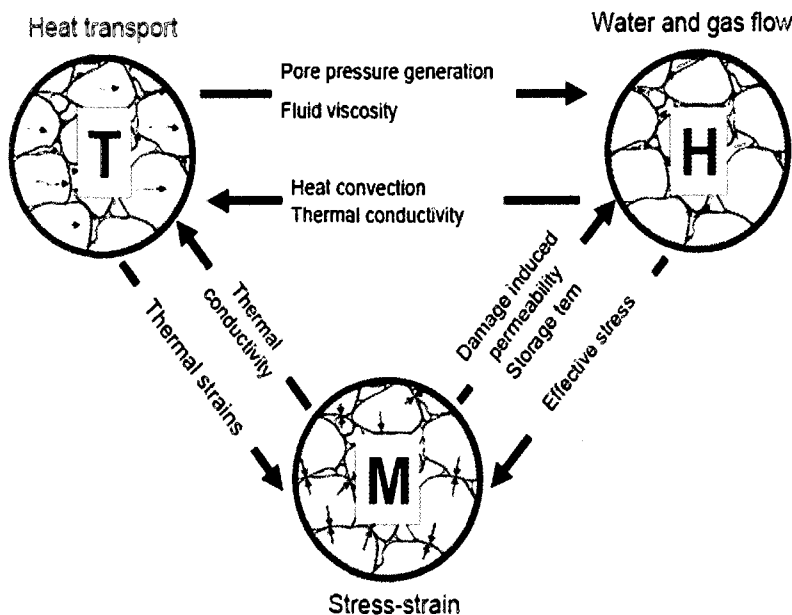


Figure 5.1 Coupled processes in a soil matrix (after Fall, 2007)

## **5.1 Thermal behaviour**

When comparing the experimental temperature results with the numerical predictions, it was observed that the thawing was taking place as anticipated in all soil samples. This section summarizes the temperature results that were obtained from the k-type thermocouples during all tests in comparison to the predicted temperature results that resulted from a thermal finite element analysis.

### **5.1.1 Analysis**

The results (Figure 3.10 and Figure 3.12) show that the soil near the surface, i.e. at the 30 cm depth, was thawing more rapidly than the others, as expected, because it was closest to the heat source. As shown in Figure 3.10, for both sample #1 and sample #2, the top sensor indicated that the thaw front had reached 30 cm after only 3.1 days of thawing. The thaw front reached 50 cm from the surface after 9.2 days of thawing. As for the bottom sensor, the thaw front had not yet reached 70 cm after 16 days of thawing, when the soil temperatures had stabilized.

It can be observed from Figure 3.12 that the thaw plane reached 30 cm from the soil surface after 2.95 days of thawing and reached 50 cm after 10.75 days of thawing for sample #3. Furthermore, the thaw plane had not reached 70 cm after the thawing period was complete as the temperature sensors were indicating a temperature of about  $-1^{\circ}\text{C}$  at this depth.

Figure 5.2 presents the temperature results obtained from the laboratory experiments after 16 days of thawing for samples #1 and #2 together with the predicted numerical results obtained from the Temp/W analysis described in section 4.1. This figure provides evidence that the Temp/W software reasonably predicted the thawing behaviour of the temperature in the permafrost soil. It is shown that the experimental data points fall inside the predicted thawing

temperature envelope that was created with the Temp/W software for the two extreme insulation cases assumed. This also provides a verification of the insulation effect of the laboratory model. The upper boundary shown in Figure 5.2 is the thawing temperature results obtained for a case where the insulating silty clay would not be surrounded by any loose-fill insulation. Whereas, the lower boundary represents the thawing temperature results for a case where the soil would have been completely insulated along the lateral surface. As the experimental results fall inside this envelope, it is understood that the lateral boundary insulation only worked to a certain extent. The experimental results for both sample #1 and sample #2 both fall closer to the lower boundary than the upper boundary of the envelope, which means that the insulation was indeed working towards minimizing the lateral boundary effects.

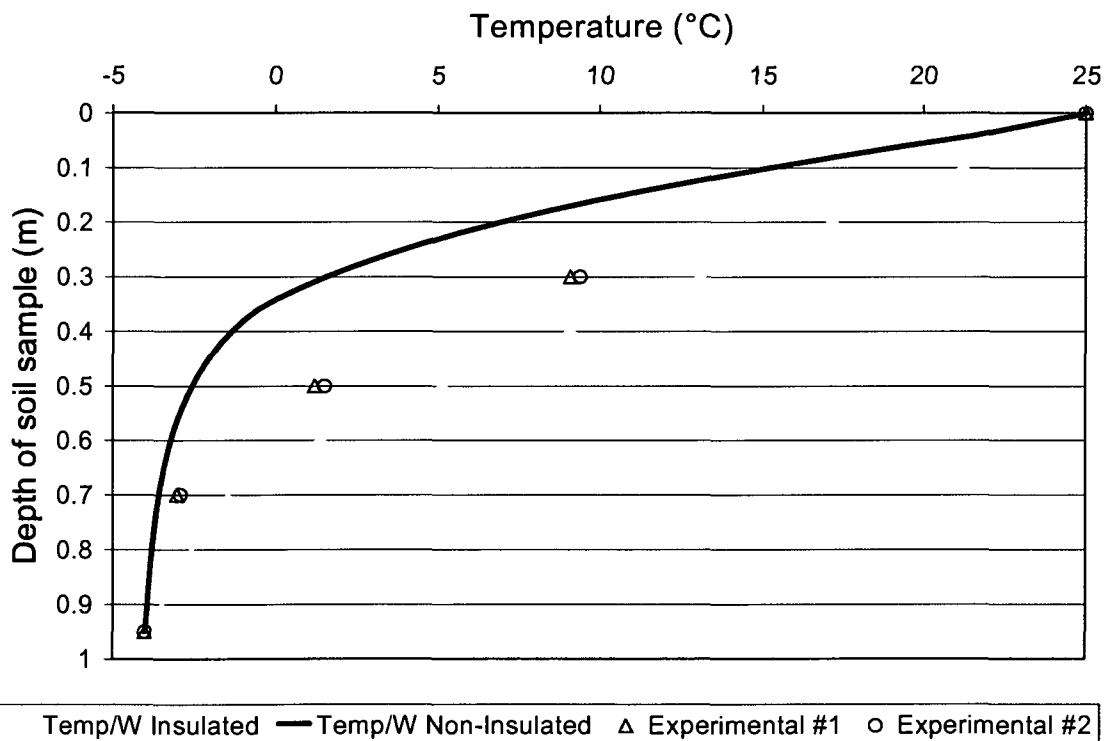


Figure 5.2 Thawing temperature envelope and results for samples #1 and #2 after 16 days of thawing

Figure 5.3 presents the temperature results obtained from the laboratory experiments after 29 days of thawing for sample #3 together with the predicted numerical results obtained from the Temp/W analysis. As was the case for the first two samples, this figure shows that the experimental data points fall inside the predicted thawing temperature envelope. Yet again, the experimental results fall inside the envelope. This indicates that the finite element software reasonably predicted the soil thawing behaviour and the insulation worked to a certain extent.

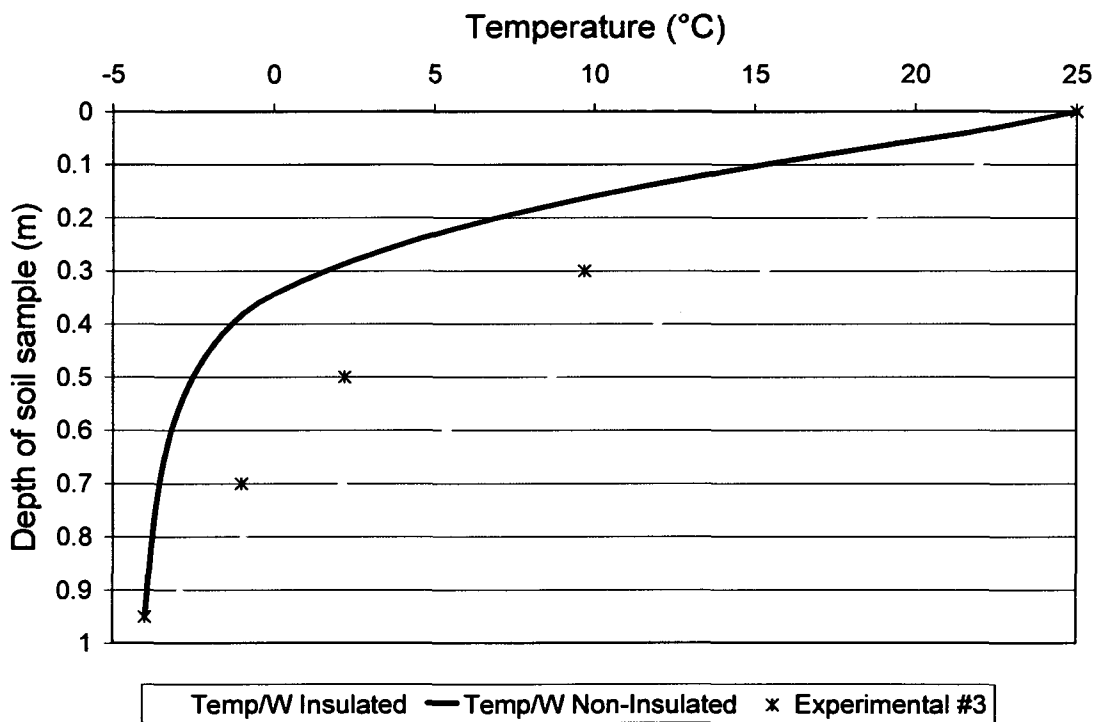


Figure 5.3 Thawing temperature envelope and results for sample #3 after 29 days of thawing

### 5.1.2 Derived thermal properties of soil samples

The time required to completely thaw a particular sample is a complex issue, which depends on many parameters, such as the diffusivity, thermal conductivity, volumetric heat capacity and volumetric latent heat of the soil, the initial ground temperature and the surface temperature (Harlan and Nixon,

1978). Equation 2.1, which estimates the position of the thaw plane, has been widely used and accepted (Carslaw and Jaeger, 1947, Morgenstern and Nixon, 1971, Morgenstern and Smith, 1973, Harlan and Nixon, 1978, Ryden, 1985). This simple solution is used here to determine the thermal constant,  $\alpha$ , of the soil samples tested.

From the temperature results presented in Figure 3.10 and Figure 3.12, the amount of time it took for the thaw front to reach 30 cm and 50 cm from the soil surface can be determined for the three series of thaw-consolidation tests. With known values of  $t$  (time) and  $X$  (depth to thaw plane), an average value of  $\alpha$  is determined for different thaw depths for a surface temperature of 25°C. The results are presented in Table 5.1. These seem to be reasonable values when comparing them to other  $\alpha$  values from the literature that have been calculated for similar soils. For example, Nixon and Ladanyi (1978) reported an  $\alpha$  value for a sample of silty clay to be 1.93 m/year<sup>1/2</sup> for a surface temperature of 10°C and a water content of 50%.

*Table 5.1 Thermal constant determination*

Sample	X (m)	t (year)	$\alpha$ (m/y <sup>1/2</sup> )
# 1	0.30	0.0082	3.3091
# 1	0.50	0.0247	3.1841
# 2	0.30	0.0082	3.3091
# 2	0.50	0.0240	3.2293
# 3	0.30	0.0079	3.3656
# 3	0.50	0.0280	2.9881

It is observed from Table 5.2 that the  $\alpha$  value is consistently higher for the soil located at 30 cm from the top of the soil column than for the soil located at 50 cm from the top. These results are reasonable based on the fact that there is faster heat penetration at the top of the soil sample, where heating is applied. Furthermore, the bottom of the soil column is open to the cold room

temperatures, therefore a slow down in heat penetration is expected near the bottom.

## **5.2 Pore water pressure**

This section discusses the pore water pressure results that were obtained from the PDCR-81 miniature pore pressure transducers during the third test and provides a comparison to the theoretical values.

### **5.2.1 Pore water pressure generation with respect to the thaw front**

While it is not clear why the upper sensor at the 30 cm depth registered extremely high suction (negative) and the lower one at the 50 cm depth registered extremely high pressure (positive) when the soil sample was frozen (Figure 3.14), both sensors responded to thawing of the sample. As shown on Figure 3.14, the upper sensor (30 cm) recorded a more rapid change of pressure than that recorded by the lower one (50 cm), when thawing reached the sensor level. This is reasonable seeing that the temperature results in Figure 3.14 provide evidence that the slope of the thawing temperatures around 0°C is higher for the sensor located at 30 cm from the soil surface than for the sensor located at 50 cm from the soil surface. Figure 5.4 presents the thaw rate when the thaw plane reached 30 cm and 50 cm from the surface, respectively. As presented in this figure, the soil located at a depth of 30 cm from the top of the soil column was thawing at a rate of 1.1°C/Day, whereas the soil located at a depth of 50 cm from the top of the soil column was thawing at a rate of 0.3°C/Day.

This would indicate that the soil located at a depth of 30 cm from the soil surface is thawing almost four times quicker than the soil that is located at a depth of 50 cm from the soil surface. This is expected since the upper sensor is closer to the heat source at the top. Thus it was taking much longer for the pore ice to turn to pore water at the lower 50 cm sensor than for the 30 cm sensor.

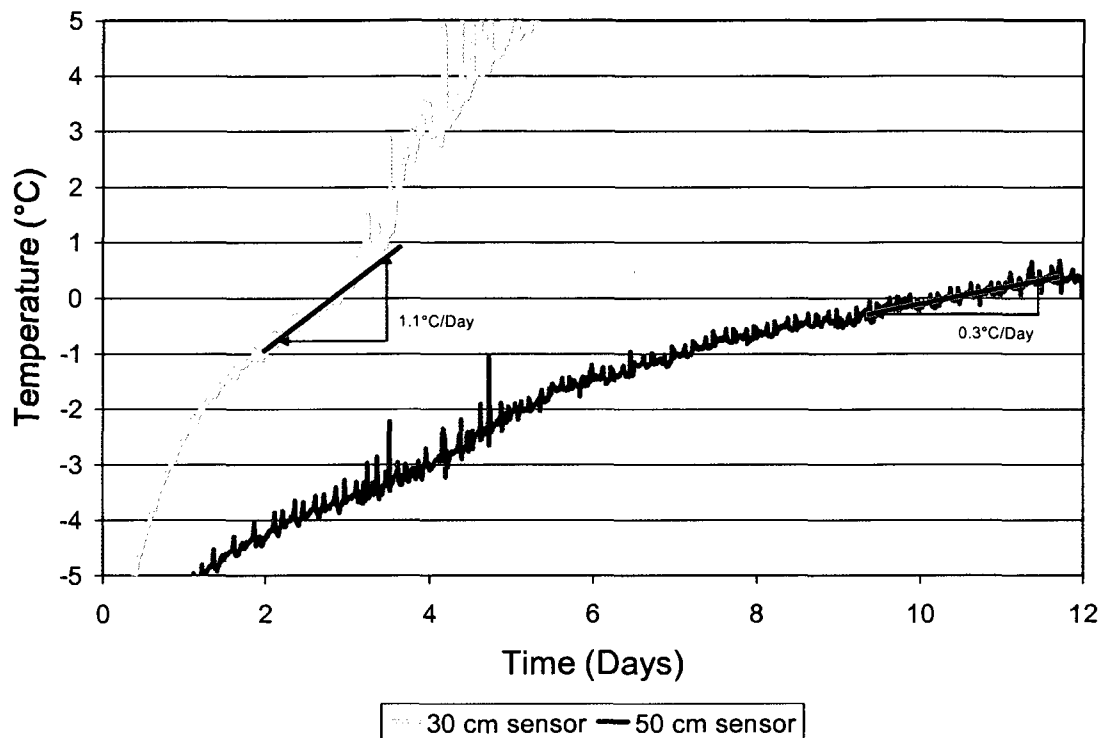


Figure 5.4 Thaw rate for two different depths

From the temperature analysis, it was found that the 0°C isotherm had reached the 30 cm sensor after 2.95 days of thawing and reached the 50 cm sensor after 10.75 days of thawing. The pressure sensors did not begin to pick up pore pressure until after 3.3 days and 14.5 days of thawing, for the sensors located at 30 cm and 50 cm depths, respectively. This is reasonable due to the ice latent heat effect.

## 5.2.2 Pore water pressure changes

### 5.2.2.1 Pore pressures at 30 cm depth

Figure 5.5 presents the pore water pressure along with the temperature readings at a depth of 30 cm from the soil surface at the beginning of the thawing stage. As shown in the figure, the pore water pressure behaviour corresponds very well to the temperature behaviour. When the temperature reached 0°C around day 3, the pressure sensors started responding rapidly. Furthermore, throughout day 3 and day 5 of thawing, the pore water pressures rose to above 0 kPa and oscillated. From the temperature results, this proves to be the time when the pore ice was turning into pore water.

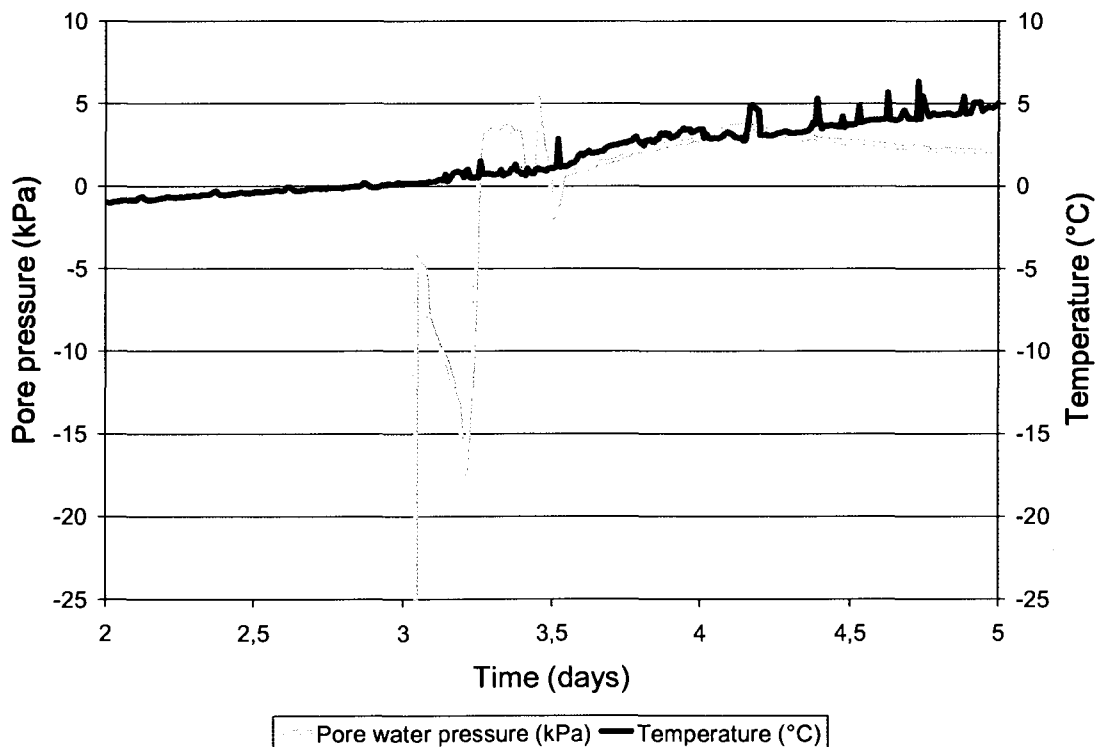


Figure 5.5 Temperature and pore water pressure readings at 30 cm depth from day 2 to day 5 of the laboratory testing

Figure 5.6 presents the pore water pressures at 30 cm depth throughout the entire thawing period. It is shown that the pore water pressures were negative at the beginning of the thawing test, while the soil and water were in the frozen state. A similar behaviour was reported by Harris and Davies (1998) who performed seven cycles of freezing and thawing tests on a silty soil. The results from one of the freeze-thaw cycles for soil located at a depth of 150 mm are presented in Figure 5.7 for comparison purposes. In order to observe the pore pressures around the previously mentioned “zero curtain period”, Figure 5.8 presents a closer look at the pore water pressure behaviour throughout day 3 and day 5 of thawing.

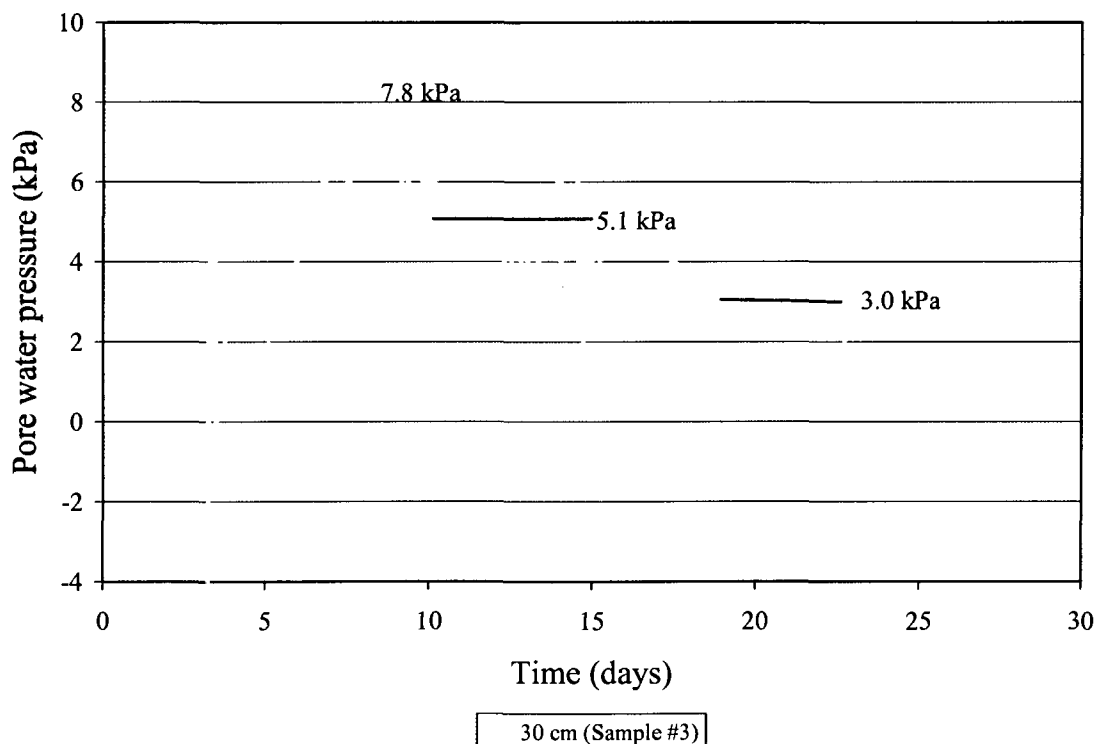


Figure 5.6 Pore water pressures at 30 cm depth

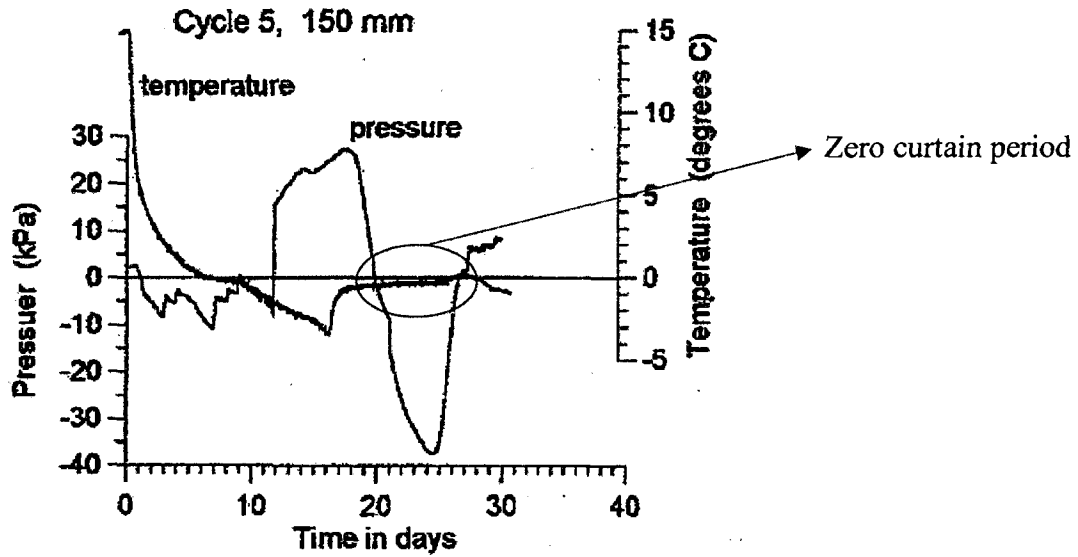


Figure 5.7 Temperature and pressure recorded during soil freezing and thawing test (after Harris and Davies, 1998)

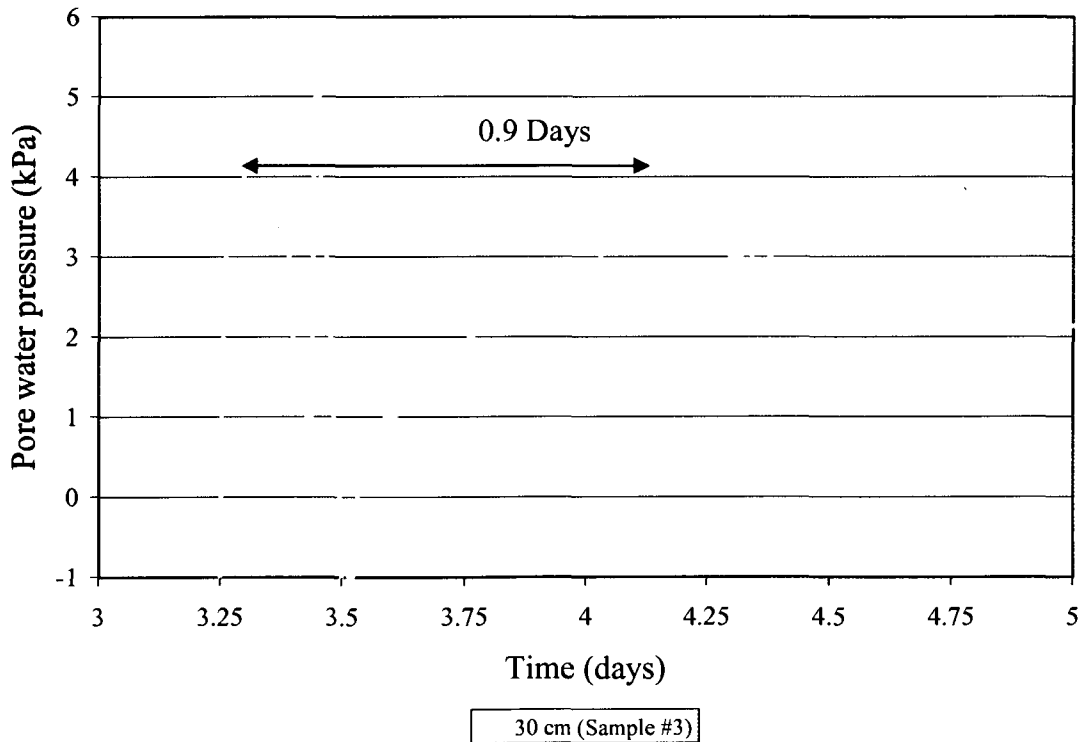


Figure 5.8 Experimental pore water pressure results for sample #3 at a depth of 30 cm

From the temperature results presented in Figure 3.12, it was determined that the thaw front had reached the 30 cm sensor after 2.95 days of thawing. Figure 5.6 confirms this fact, as the pressure sensors responded shortly after 2.95 days of thawing. The pressure first peaked at day 3.3. It is observed from Figure 5.8 that during the first day after the temperature reached 0°C, the pore water pressures reached a first peak, then fall below zero, peak again to a higher value, dropped below zero again before slowly increasing to about the same value as the first peak. This depicts the behaviour of the pore water pressures during the zero curtain period as presented by Harris and Davies (1998). This pore pressure behaviour indicates that, even though the temperature results showed temperatures of +0°C to +4°C from day 3.3 to day 4.2 of thawing, there could still be pore ice in the soil.

As shown in Figure 5.6, the pore water pressures continued to rise, and oscillated up and down until about 8.75 days into the thawing process when a maximum pore pressure of around 7.8 kPa was picked up. It is unclear whether this high pore water pressure is related to possible existence of pore ice. Following this peak, the pore water pressures began to decrease, which is expected as they were allowed to dissipate and evaporate through the surface of the soil column. There was a period, from day 10 to day 15 of thawing, where the average pore water pressure is about 5.1 kPa. This corresponds to the overburden pressure applied by the saturated silty clay at a depth of 30 cm.

As thawing progressed, the pore water pressures continued to decrease. From day 19 to day 22.5 of thawing, the average pore water pressure was about 3.0 kPa. This corresponds to the hydrostatic pressure at 30 cm depth. It means that the excess pore water pressure has fully dissipated by then. It was unclear why there was a sudden drop of pore pressure after the excess pore water pressure was fully dissipated. However, the pore water pressure is expected to drop further due to evaporation with time. At the end of the test, a crust was observed at the top of the soil.

### 5.2.2.2 Pore pressures at 50 cm depth

From the temperature results (Figure 3.12), it was determined that the thaw front had reached the 50 cm sensor after 10.75 days of thawing. It is observed from Figure 3.14 that the pressure sensor at 50 cm depth started responding to the temperature increase at around day 5, when the temperature increased to about  $-2^{\circ}\text{C}$  (Figure 3.12). A closer look of the pressure chart is reproduced in Figure 5.9. It is noted that the pressure dropped sharply to a more reasonable level of 7.4 kPa at about day 14.5. This is about 4 days after the temperature reached  $0^{\circ}\text{C}$  at this depth. The temperature slowly crept up thereafter to slightly above  $+2^{\circ}\text{C}$  throughout the remaining part of the test. It is suspected that, with this temperature, some pore ice may still exist. This probably explains why the water pore pressure continued oscillating, which mimicked the “zero curtain” effect (Harris and Davies, 1998).

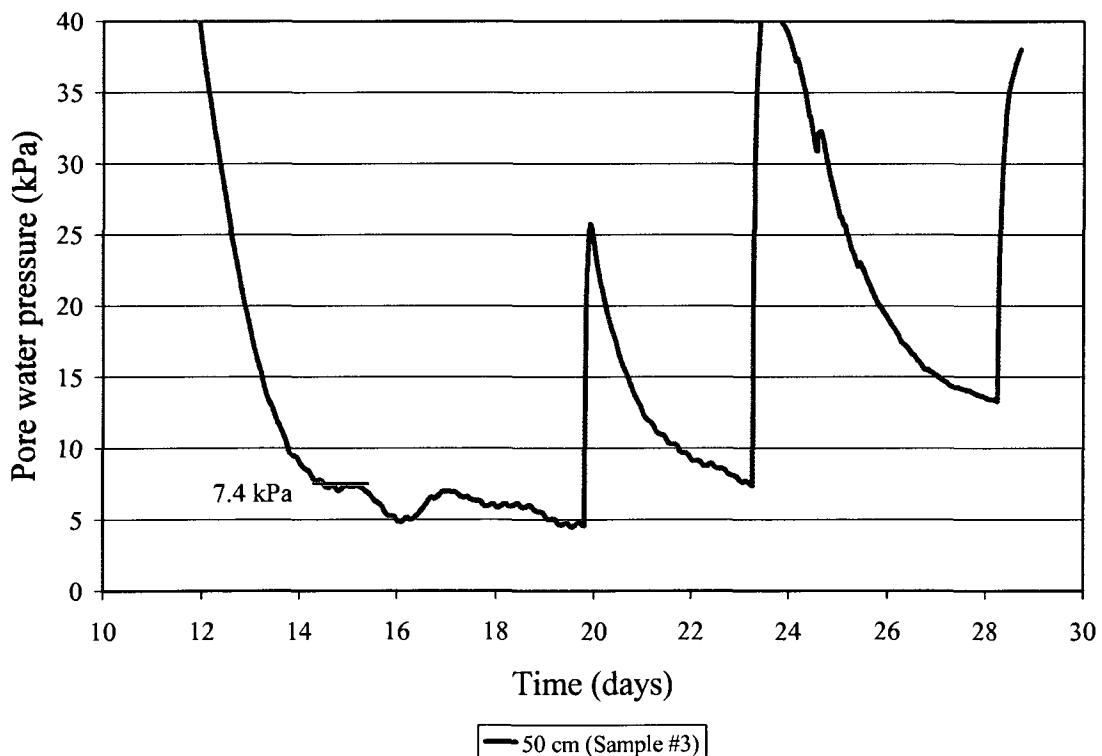


Figure 5.9 Pore water pressures at 50 cm from soil surface

Nonetheless, the pore water pressure of 7.4 kPa between day 14.5 and day 15.5 of thawing was checked against the overburden pressure, which is about 9.1 kPa, and the hydrostatic pressure, which is about 5 kPa, assuming the soil was still fully saturated throughout the column above. The measured value of 7.4 kPa falls within this range, thus making it a reasonable outcome as the soil was unsaturated at the top and the consolidation process had begun.

### ***5.2.3 Remarks on accuracy of measured data***

Careful consideration must be taken when interpreting the test data and comparing the temperature results with the pore water pressure results because both sensors are subject to a number of things that may affect the results, such as instrumental error, location, behavior of the soil, etc. The thermocouples and pressure transducers were placed side by side, however, these sensors could have been slightly displaced. Even though the temperature sensors picked up a temperature of  $+0^{\circ}\text{C}$ , the exact time when the thaw front reached the sensor is questionable due to the accuracy of the sensor and due to the complex physical behaviour of water, ice and soil within a zone of  $\pm 0^{\circ}\text{C}$ . Since a temperature of  $0^{\circ}\text{C}$  represents the melting point of the ice as well as the freezing point of water. The shaft friction between the soil and the pvc column may also affect the pressure. A teflon spray was applied on the interior of the pvc pipe to reduce friction, however the effectiveness of this method was not measured during the laboratory experiment. Furthermore, the pressure sensors may be affected by temperature change as well. Consequently, any discrepancies between the readings can be due to a combination of the accuracy of the sensors, the differences in the temperature and pressure sensor locations, and the thickness of the transition zone around the  $0^{\circ}\text{C}$  isotherm where pore ice may exist.

#### **5.2.4 Comparison of pore pressure data with theoretical results**

The laboratory test data are compared with the theoretical results from Equation [2.3] developed by Morgenstern and Nixon (1971). As there was no load applied to the soil surface during the laboratory procedures,  $P_o$  is equal to zero, thus the complete solution is reduced to the following equation:

$$u(x,t) = \frac{\gamma' x}{1 + \frac{1}{2R^2}} \quad [5.1]$$

The respectful excess pore water pressures can therefore be calculated from Equation [5.1] for the two depths,  $x$ , measured in the laboratory, 30 cm and 50 cm from the soil surface. The thaw consolidation ratio is calculated with Equation [2.4] based on the coefficient of consolidation range given in Table 3.3 and the  $\alpha$  values calculated in Table 5.1. The range of excess pore water pressure calculated for each depth are given in Table 5.2. Those values are also plotted in Figure 5.10, along with the excess pore water pressure values measured experimentally.

The excess pore water pressures calculated from Equation [5.1] are a function of the submerged unit weight of the soil, the depth at which the excess pore water pressures are measured and of the thaw consolidation ratio. This equation represents the initial value of excess pore water pressure that is generated at the moment when the pore ice changes to water. Figure 5.10 provides experimental evidence that excess pore water pressures are generated at a depth of 30 cm and 50 cm below the ground surface when the thaw plane reaches the respective depth. It can be observed from the preceding figure that the excess pore pressures were 2.69 kPa for the 30 cm sensor and 2.45 kPa for the 50 cm sensor after 3.45 days and 15.00 days of thawing, respectively. The experimental pore water pressures obtained at the two different depths fell within

the region of the predicted excess pore pressure range calculated from Equation [5.1].

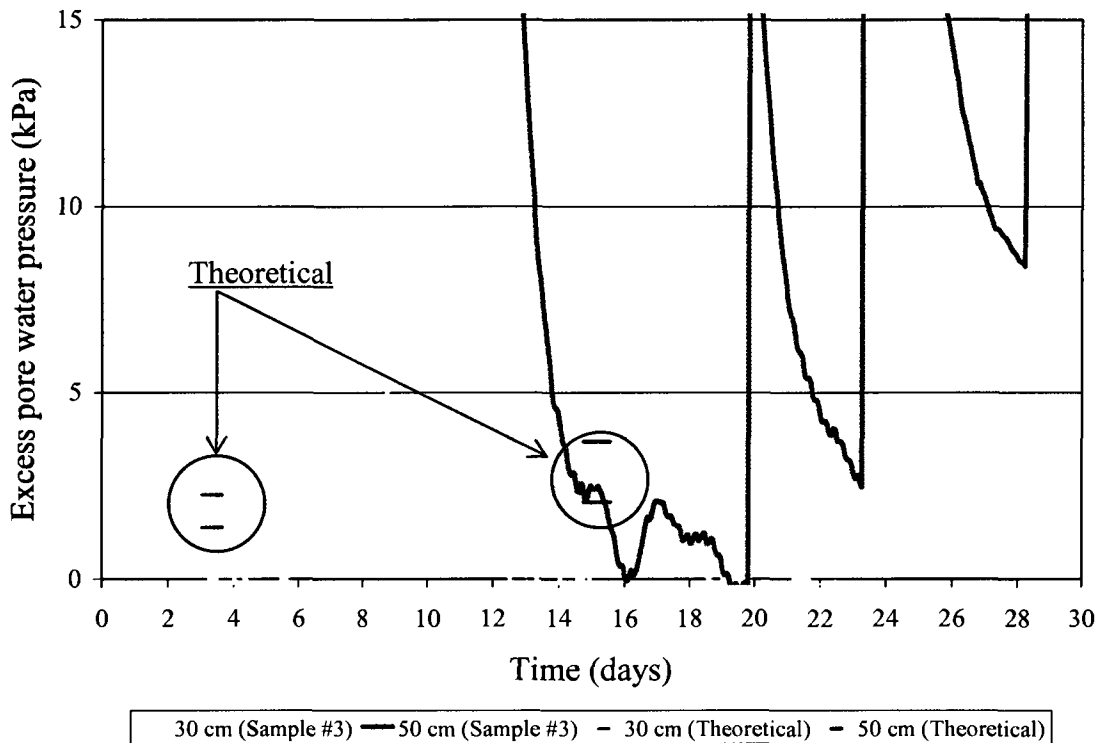


Figure 5.10 Theoretical and experimental excess pore water pressure

It should be noted that the theoretical values assume that pore ice changes to pore water instantly when the thaw front reaches the depth of interest. In reality, there is always a transition zone where pore ice changes to water gradually. During this progressive thawing process, part of the upper layer soil may have become unsaturated. In other words, the water table at the soil surface, that is used for calculating the excess pore water pressure, may not be correct. Given above discrepancies, it is considered that the theoretical and experimental results are reasonably agreeable.

### 5.3 Moisture migration

This section analyzes the moisture contents measured during the laboratory experiment with respect to the moisture migration predicted from the Vadose/W numerical analysis. Figure 5.11 presents the volumetric moisture content measured within the silty clay soil in sample #1 and sample #2 after 16 days of thawing, along with the moisture content predicted by the finite element model. Similarly, Figure 5.12 presents the volumetric moisture content measured within the soil in sample #3 after 29 days of thawing, along with the moisture content predicted by the numerical model.

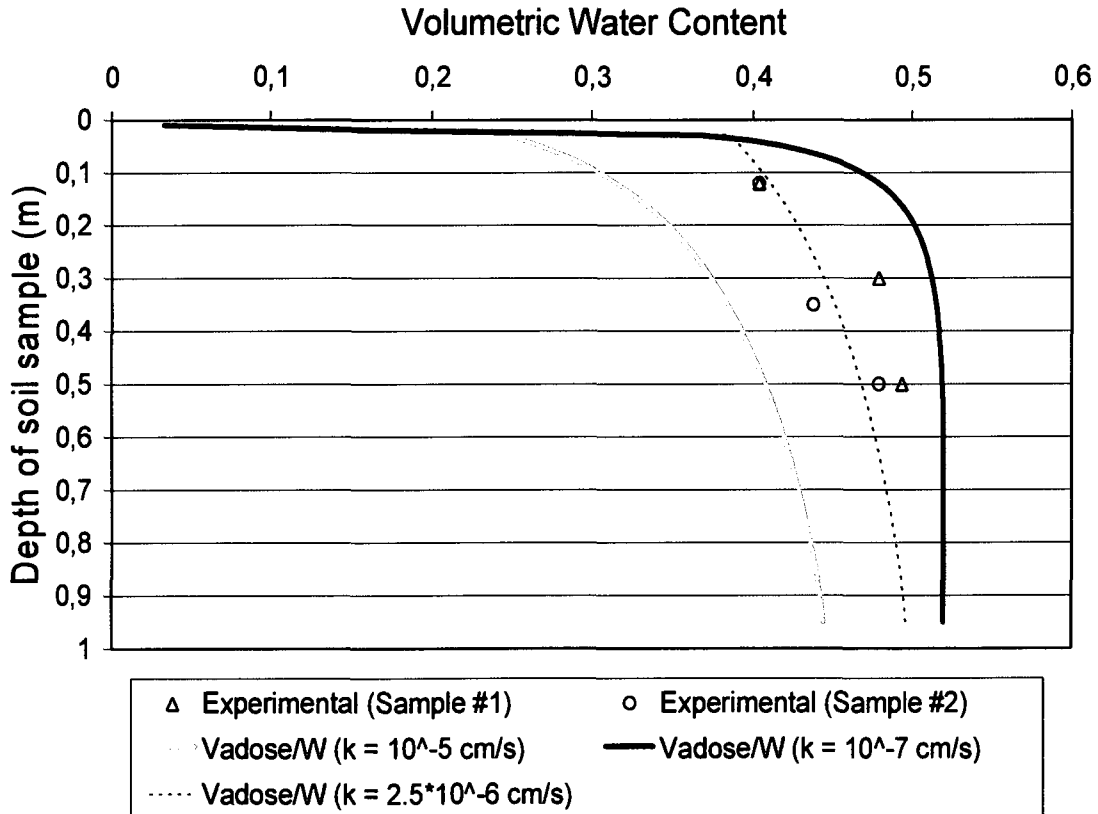


Figure 5.11 Experimental and theoretical moisture contents after 16 days of thawing

Both figures present an upper bound case and a lower bound case corresponding to the hydraulic conductivity values assumed as discussed in

section 4.2.1. Furthermore, the dotted curve represents the results with a hydraulic conductivity that best suited the experimental data.

As can be observed from these two figures, the finite element software, Vadose/W, was able to predict the moisture conditions successfully for the three samples tested.

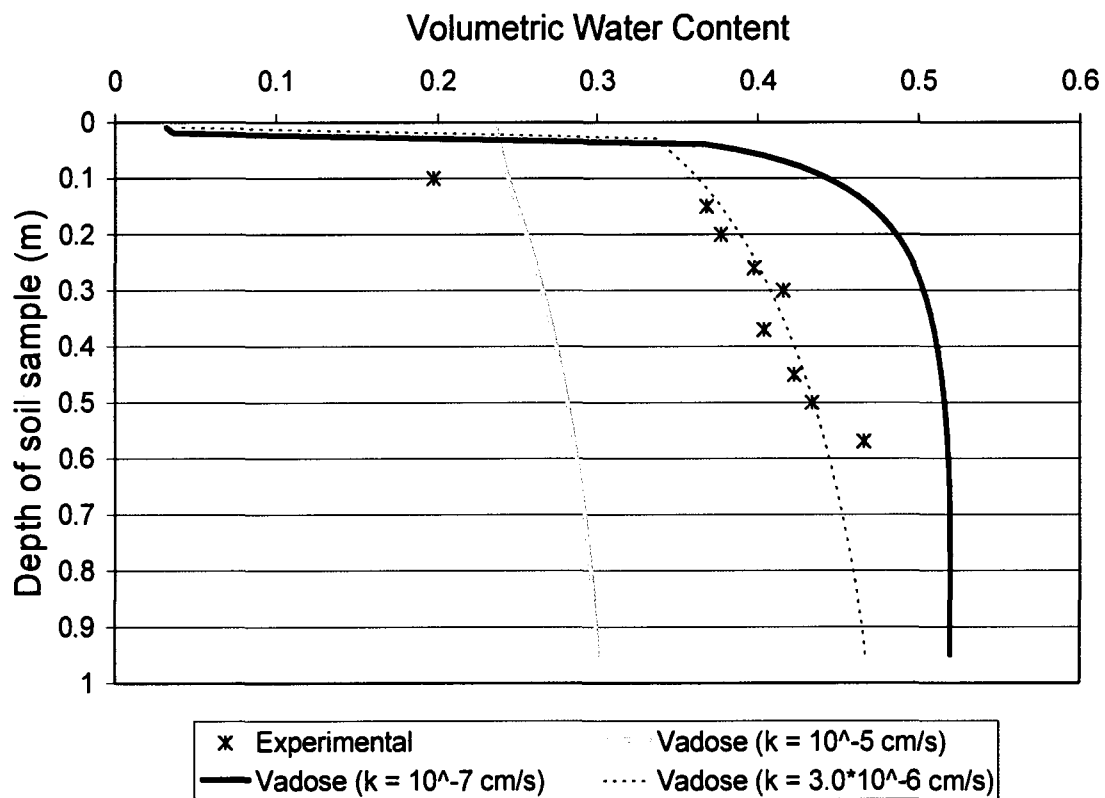


Figure 5.12 Experimental and theoretical moisture migration after 29 days of thawing

Furthermore, information can be derived from the shape of the curves. At the top of the soil column, the soil is relatively dry after 16 and 29 days of thawing. This drying is a result of evaporation. The potential evaporation was measured to be 8 mm/day for the thawing scenario set up in the laboratory. As thawing proceeded and the soil dried, a crust formed at the top of the soil column. Due to this reason, it should be noted that care must be taken when estimating the

hydrostatic pressure, with respect to the excess pore water pressure interpretation.

Finally, it appears that the sample tested in the laboratory is more closely following the thawing pattern of the finite element model having a saturated hydraulic conductivity of  $1 \times 10^{-7}$  cm/s. From the results presented by the dotted curve on both figures, it would be reasonable to state that the silty clay soil sample used for testing has a saturated hydraulic conductivity of around  $2.5 \times 10^{-6}$  cm/s to  $3.0 \times 10^{-6}$  cm/s.

## 6 Conclusion

A large-scale laboratory device was developed to verify the temperature, pore water pressure and moisture migration behaviour of thawing soils. Finite element models were developed to simulate the conditions set up in the laboratory and to predict the thermal and hydraulic behaviour of the soil samples. The results obtained from three thawing tests were analyzed in comparison to numerical predictions obtained from the finite element modeling as well as to theoretical predictions calculated from the thaw consolidation theory developed by Morgenstern and Nixon (1971).

It was observed from the temperature results that heat penetration was faster at the top of the soil column than at the bottom due to difference of thermal gradient. When comparing the experimental results with the results obtained from the thermal finite element modeling, it was found that the designed laboratory equipment was capable of simulating the temperature behaviour with reasonable accuracy for a silty clay soil. Furthermore, through the finite element analysis, it was determined that the insulation surrounding the soil column was only working to a certain extent. If this test were to be repeated, an improved insulation system should be used to surround the soil columns in order to ensure that the soil is thawing more uniformly from the top down, as would occur in natural ground thawing conditions in permafrost regions.

As for the analysis of the moisture migration, both the experimental and numerical results followed the same pattern, therefore the designed laboratory equipment was again shown capable of simulating natural field conditions for the purpose of verifying the thaw consolidation theory. After the thawing process was complete, the moisture content at the top of the soil columns was low and a crust was formed due to evaporation. The thaw consolidation theory assumes that the soil above the thaw front is saturated. However, as measured in the laboratory, the upper portion of the soil column became unsaturated during the

thaw consolidation process. Therefore, care must be taken when calculating the hydrostatic pressure necessary for determining the excess pore water pressures. During the laboratory test it was also observed that the moisture content increased with depth and approached the initial volumetric moisture content at the depth of the thaw plane. As thaw consolidation occurs, the void ratio is changing throughout the soil column, thus inducing a related change in water content.

When comparing the temperature measurements to the pore water pressure measurements, it was found that the pore water pressure fluctuations corresponded to the temperature changes, especially around the “zero curtain period” zone. However, as the thaw plane progressed, the pore water pressures fluctuated and, at times, reached high peaks, especially in near the sensor located at 50 cm from the soil surface. It is not certain why the pore pressures fluctuated so much, however it can be due to many factors, such as possible existence of pore ice, shaft resistance, and the sensor accuracy. It was observed from the laboratory results that there is a phase change zone around the 0°C isotherm. Thus, when the thaw line reaches a certain depth, only a portion of the ice turns to water at that depth. When comparing the theoretical predictions to the experimental results, it must be understood that some of the pore water pressures at the thaw front have time to dissipate while the rest of the ice is melting.

Given all the uncertainties and discrepancies mentioned above, the experimental pore water pressures and the theoretical results from the thaw consolidation theory by Morgenstern and Nixon (1971) compared reasonably well for a case where the thawing soil is consolidated by its own weight. However, further development of the thaw consolidation theory is necessary to take into account the phase change zone as well as the unsaturated zone.

## References

- Aylsworth, J. M., Burgess, M. M., Desrochers, D.T., Duk-Rodkin, A., Robertson, T. & Traynor, J.A. (2000). Surficial geology, subsurface materials, and thaw sensitivity of sediments. In Dyke, L.D. & Brooks, G.R. (Eds.), *The physical environment of the Mackenzie valley, Northwest Territories: A base line for the assessment of environmental change* (pp. 41-48). Canada: Geological Survey of Canada, Bulletin 547.
- Aylsworth, J. M., Duk-Rodkin, A., Robertson T., & Traynor, J.A. (2000) Landslides of the Mackenzie Valley and adjacent mountainous and coastal regions. In Dyke, L.D. & Brooks, G.R. (Eds.), *The physical environment of the Mackenzie valley, Northwest Territories: A base line for the assessment of environmental change* (pp. 167-176). Canada: Geological Survey of Canada, Bulletin 547.
- Andersland, O. B. & Anderson, D. M. (1978). *Geotechnical engineering for cold regions*. United States of America: McGraw-Hill Book Company. 566 pp.
- Brown, R. J. E. & Kupsch, W. O. (1974). *Permafrost terminology*. Canada: National Research Council, Associate Committee Geotechnical Research, Tech. memo. 111.
- Carlsaw, H. S. & Jaeger, J. C. (1947). *Conduction of heat in solids*. Oxford: Clarendon Press.
- Craig, R. F. (2004). *Craig's soil mechanics*. New York, United States of America: Spon Press. 447 pp.
- Das, B. M. (2004). *Principles of foundation engineering*. Pacific Grove, United States of America: Brooks/Cole-Thompson Learning. 743 pp.

Dyke, L. D., (2000). Climate of the Mackenzie River valley. In Dyke, L.D. & Brooks, G.R. (Eds.), *The physical environment of the Mackenzie valley, Northwest Territories: A base line for the assessment of environmental change* (pp. 21-30). Canada: Geological Survey of Canada, Bulletin 547.

Eigenbrod, K. D., Knutsson, S. & Sheng, D. (1996). Pore-water pressures in freezing and thawing fine-grained soils. *Journals of Cold Regions Engineering, Vol. 10, No. 2*, pp. 77-92.

Environment Canada (2007). Climate data. Retrieved February 5, 2007, from [http://climate.weatheroffice.ec.gc.ca/climateData/canada\\_e.html](http://climate.weatheroffice.ec.gc.ca/climateData/canada_e.html)

Fall, M. (2007). *Geotechnical Hazards*. Course notes from University of Ottawa Geotechnical Hazards course CVG6303, University of Ottawa, Canada.

Geological Survey of Canada (2007). Permafrost; Communities and climate change. Retrieved April 11, 2008, from [http://gsc.nrcan.gc.ca/permafrost/communities\\_e.php](http://gsc.nrcan.gc.ca/permafrost/communities_e.php).

Geo-Slope International Ltd. (2007a). *Thermal modeling with TEMP/W – An engineering methodology*. Alberta, Canada: TEMP/W Software User's Manual from Geo-Slope International Ltd., Second Edition. 240 pp.

Geo-Slope International Ltd. (2007b). *Vadose zone modeling with VADOSE/W – An engineering methodology*. Alberta, Canada: Vadose/W Software User's Manual from Geo-Slope International Ltd., Second Edition. 334 pp.

Global warming art (2007). Instrumental temperature record. Retrieved March 6, 2007, from <http://www.globalwarmingart.com/>

- Goodrich, L. E. (1982). The Influence of snow cover on the ground thermal regime. *Canadian Geotechnical Journal*, Vol. 19, pp. 421-432.
- Government of Canada (2004). Climate change. Retrieved February 16, 2007, from [http://www.climatechange.gc.ca/english/climate\\_change](http://www.climatechange.gc.ca/english/climate_change).
- Harlan, R. L. & Nixon J. F. (1978). Ground thermal regime. In O. B. Andersland & D. M. Anderson (Eds.), *Geotechnical engineering for cold regions* (pp. 103-163). United States of America: McGraw Hill Book Company.
- Harris, C., Davies, M. C. R. & Coutard, J.-P. (1995). Laboratory simulation of periglacial solifluction: significance of porewater pressure, moisture contents and undrained shear strengths during soil thawing. *Permafrost and periglacial processes*, Vol. 6, pp. 293-311.
- Harris, C. & Davies, M. C. R. (1998). Pressures recorded during laboratory freezing and thawing of a natural silt-rich soil. *Proceedings of the 7<sup>th</sup> international conference on permafrost, Collection Nordicana No. 55*, pp. 433-439.
- Harris, C., Rea, B. R. & Davies, M. C. R. (2001). Scaled physical modelling of mass movement processes on thawing slopes. *Permafrost and periglacial processes*, Vol. 12, pp. 125–135.
- Harris, C., Davies, M. C. R. & Rea, B. R. (2003). Gelifluction; viscous flow or plastic creep, *Earth surface processes and landforms*, Vol. 28, pp. 1289-1301.
- Houghton, J. T., Ding, Y., Griggs, D. J., Noguera, M., Van Der Linden, P. J., Dai, X, Maskell, K. & Johnson, C. A. (2001). *Climate change 2001: The scientific basis*. Cambridge, UK: Cambridge University Press. 881 pp.

- Intergovernmental Panel on Climate Change (IPCC) (2007). *Climate change 2007: The physical science basis*. IPCC WGI Fourth Assessment Report, Summary for Policymakers, 21 pp.
- Isaacs, R. M. (1974). *Geotechnical studies of permafrost in the Fort Good Hope - Norman Wells region, NWT*, Environmental-Social Committee on Northern Pipelines, Task Force on Northern Oil Development, Report No. 74-16.
- Johnston, G. H. (1981), *Permafrost, engineering design and construction*, Canada: National Research Council, Associate Committee Geotechnical Research.
- Kersten, M. S. (1948). *Laboratory research for the determination of the thermal properties of soils*. University of Minnesota: U.S. Army Corps of Engineers. 90 pp.
- Konrad, J. M. & Roy, M. (2000). Flexible pavements in cold regions: a geotechnical perspective. *Canadian Geotechnical Journal*, Vol. 37, pp. 689-699.
- Lee, I. K., White, W. & Ingles, O. G. (1983). *Geotechnical engineering*, Boston, USA: Pitman.
- Lewkowicz, A.G. (1992). A solifluction meter for permafrost sites, *Permafrost and Periglacial Processes*, Vol.3, pp. 11-18.
- Luscher, U. & Afifi-Sherif, S. (1973). Thaw consolidation of Alaskan silts and granular soils. *Permafrost; North American Contribution, Second International Conference; Physics, Physical Chemistry, and Mechanics of Frozen Ground and Ice*, pp. 325-334.

- McRoberts, E. C. (1978). Slope stability in cold regions. In O. B. Andersland & D. M. Anderson (Eds.), *Geotechnical engineering for cold regions* (pp. 363-404). United States of America: McGraw Hill Book Company.
- McRoberts, E. C. & Morgenstern, N. R. (1974). The stability of thawing slopes. *Canadian Geotechnical Journal*, Vol. 11, pp. 447-469.
- McRoberts, E. C. & Morgenstern, N. R. (1975). Pore water expulsion during freezing. *Canadian Geotechnical Journal*, Vol. 12, pp. 130-141.
- Morgenstern, N. R. & Nixon, J. F. (1971) One-dimensional consolidation of thawing soils. *Canadian Geotechnical Journal*, Vol. 8, pp. 558-565.
- Morgenstern, N. R. & Smith, L. B. (1973). Thaw-consolidation tests on remoulded clays. *Canadian Geotechnical Journal*, Vol. 10, pp. 25-39.
- Muller, S. W. (1947). *Permafrost of permanently frozen ground and related engineering problems*. Ann Arbor, Michigan: Edwards Bros. 231 pp.
- Muraleetharan, K. K. & Granger, K. K. (1999). The use of miniature pore pressure transducers in measuring matric suction in unsaturated soils. *Geotechnical Testing Journal*, Vol. 22, No. 3, pp. 226-234.
- Murton, J. B. & Harris, C. (2003). *The experimental simulation of ice-wedge casting*, In Phillips, M., Springman, S. M. & Arenson, L. U. (Eds.), *Proceedings of the eighth international conference on permafrost* (pp. 807–810). Zurich: Swets & Zeitlinger.

- Nixon, F. M. (2000). Thaw-depth monitoring. In Dyke, L.D. & Brooks, G.R. (Eds.), *The physical environment of the Mackenzie valley, Northwest Territories: A base line for the assessment of environmental change* (pp. 119-126). Canada: Geological Survey of Canada, Bulletin 547.
- Nixon, J. F. (1973). Thaw-consolidation of some layered systems. *Canadian Geotechnical Journal*, Vol. 10, pp. 617-631.
- Nixon J. F. & Ladanyi, B. (1978). Thaw consolidation. In O. B. Andersland & D. M. Anderson (Eds.), *Geotechnical engineering for cold regions* (pp. 164-215). United States of America: McGraw Hill Book Company.
- Nixon, J. F. & Morgenstern, N. R. (1974). Thaw-consolidation tests on undisturbed fine-grained permafrost. *Canadian Geotechnical Journal*, Vol. 11, pp. 202-214.
- Nixon, J. F. & Pick, A. R. (1985). Design of Norman Wells pipeline for frost heave and thaw settlement. *Proceedings on the workshop on Subsea Permafrost and Pipelines in Permafrost, National Research Council of Canada, Technical Memo 139*, pp. 67-85.
- Nelson, R. A., Luscher, U., Rooney, J. W. & Stramier, A. A. (1983). Thaw strain data and thaw settlement predictions for Alaskan soils. *Proceedings of the fourth international conference on permafrost*, Vol. 4, pp. 912-917.
- Penner, E. (1970). Thermal conductivity of frozen soils. *Canadian Journal of Earth Sciences*, Vol. 7, pp. 982-987.
- Riseborough, D. W. (2002). The mean annual temperature at the top of permafrost, the TTOP model, and the effect of unfrozen water. *Permafrost and periglacial process*, Vol. 13, pp. 137-143.

- Ryden, C. G. (1985). Pore pressure in thawing soil. *Proceedings of the fourth international symposium on ground freezing, Vol.5, No. 7*, pp. 223-226.
- Saarelainen, S. (1999). Thaw-weakening of frost-susceptible subgrades. *Proceedings of the twelfth European conference on soil mechanics and geotechnical engineering: geotechnical engineering for transportation infrastructure; theory and practice, planning and design, construction and maintenance, Vol. 12, No. 2*, pp. 1353-1358.
- Savigny, W., Logue, C. & MacInnes, K. (1995). Forest fire effects on slopes in ice-rich permafrost soils, Mackenzie Valley, NWT. *Proceedings of the forty-eighth Canadian geotechnical conference, Preprint Vol. 2*, pp. 989-998.
- Shur, Y., Hinkel, K.M. & Nelson, F.E. (2005). The Transient layer : Implications for geocryology and climate-change science. *Permafrost and Periglacial Processes Vol. 16*, pp.5-17.
- Smith, L. B. (1972). *Thaw-consolidation tests on remoulded clays*. Edmonton, Alberta: M.Sc. thesis, University of Alberta. 157 pp.
- Smith, M. W. & Riseborough, D. W. (1985). The sensitivity of thermal predictions to assumptions in soil properties. *Proceedings of the fourth international symposium on ground freezing, Vol.5, No. 7*, pp. 17-23.
- Su, X., Wang, B. & Nichol, S. (2006). Back analysis of a slope failure in permafrost in the Mackenzie valley, Canada. *Proceedings of the thirteenth international conference on cold region engineering, Vol. 210*, pp. 50.

- Sutherland, H. B. & Gaskin, P. N. (1973). Pore water and heaving pressures developed in partially frozen soils. *Proceedings of the second international conference on permafrost*, Publication 2115, pp. 409-419.
- Tarnawski, V. R. & Wagner, B. (1993). Modeling the thermal conductivity of frozen soils. *Cold Regions Science and Technology*, Vol. 22, pp. 19-31.
- Terzaghi, K., Peck, R. B. & Mesri, G. (1996). *Soil mechanics in engineering practice*, John Wiley & Sons, New York, 616 pp.
- Tsyтович, N. A. (1960). *Bases and foundations on frozen soils*. Washington, D. C.: Spec. Rep. 58, Highway Research Board, National Academy of Sciences.
- UK Climate research unit (2007). Temperature. Retrieved March 6, 2007, from <http://www.cru.uea.ac.uk/cru/data/temperature/>
- US Army Corps of Engineers (1995). *Engineering and design - Instrumentation of embankment dams and levees. United States of America: U.S. Army engineer manual*, Chapter 2.
- U.S. Department of the Navy (1971). *Soil mechanics, foundations, and earth structures*, NAVFAC design manual DM-7, Washington, DC.
- Wang, B. & Lesage, K. (2007). Impact of climate change on slope stability in permafrost regions. *Proceedings of the 8th International Symposium on Cold Region Development*, Tampere, Finland, September 2007.
- Wang, B., Nichol S. & Su, X. (2005). Geotechnical field observations of landslides in fine-grained permafrost soils in the Mackenzie Valley, Canada. In K. Sassa, H. Fukuoka, F. Wang & G. Wang (Eds.), *Proceedings of the First General Assembly of the International Consortium on Landslides*, Chapter 25, pp. 203-212.

- Wang, B. & Saad, B. (2007). In-situ measurements of ground response to heat penetration induced by removal of organic cover in fine-grained permafrost soils. *Proceedings of the first North American landslide conference*, pp. 1595-1604.
- Williams, P. J. & Smith, M. W. (1991). *The frozen earth. Fundamentals of geocryology*. Cambridge, UK: Cambridge University Press.
- Wu, Q. & Tong, C. (1991). Thaw-consolidation process and calculation of frozen clayey soil. *Proceedings of the sixth international symposium on ground freezing, Vol. 6*, pp. 89-92.
- Zoltai, S. C. & Pettapiece, W. W. (1973). *Terrain, vegetation and permafrost relationships, Northern Mackenzie valley and Yukon*. Environmental-Social Committee on Northern Pipelines, Task Force on Northern Oil Development, Report No. 73-4.

## Appendix A – Thaw consolidation theory

Morgenstern and Nixon (1971) presented the following derivation for their thaw consolidation theory, starting with the movement of the thaw plane, given by the Newmann solution:

$$X(t) = \alpha\sqrt{t} \quad [1]$$

Where  $a$  = constant determined in the solution of the heat conduction problem  
 $X$  = distance to the thaw plane from the soil surface  
 $t$  = time

In the thawed region, it is assumed that the soil is compressible and that the theory of consolidation is valid.

$$c_v \frac{\partial^2 u}{\partial x^2} = \frac{\partial u}{\partial t} - \frac{\partial \sigma}{\partial t} \quad [2]$$

Where  $u$  = excess pore pressure  
 $x$  = depth measured from the ground surface  
 $\sigma$  = total stress applied  
 $c_v$  = coefficient of consolidation

If the stress does not vary with time, the equation becomes:

$$c_v \frac{\partial^2 u}{\partial x^2} = \frac{\partial u}{\partial t} \quad [3]$$

Boundary Conditions:

$$t = 0; \quad X = 0 \quad [4]$$

$$t > 0; \quad u = 0; \quad x = 0 \quad [5]$$

From Darcy's Law, the volume of pore fluid expelled from a small layer  $\Delta X$  as the thaw line advances through an increment in time  $\Delta t$  is

$$\Delta V = -\frac{Ak \frac{\partial u}{\partial x}(X, t)}{\gamma_w} \Delta t \quad [6]$$

Where  $\Delta V$  = discharge  
 $A$  = cross-sectional area of a soil element  
 $k$  = hydraulic conductivity of the soil  
 $\frac{\partial u}{\partial x}(X, t)$  = excess pore pressure gradient at the thaw interface  
 $\gamma_w$  = unit weight of water

The discharge is equal to the change in volume of a layer of thickness  $\Delta X$ . The volumetric strain is given by

$$\frac{\Delta V}{V} = \frac{\Delta V}{A\Delta X} = -\frac{k \frac{\partial u}{\partial x}(X, t)}{\gamma_w \frac{dX}{dt}} \quad [7]$$

For a compressible soil:

$$\frac{\Delta V}{V} = -m_v \Delta \sigma' \quad [8]$$

Where  $m_v$  = coefficient of volume compressibility

From Equations [7] and [8]

$$\Delta \sigma' = \frac{c_v \frac{\partial u(X,t)}{\partial x}}{\frac{dX}{dt}} \quad [9]$$

The total stress at  $x = X$  is:

$$\sigma(X,t) = P_0 + \gamma X \quad [10]$$

Where  $P_0$  = load applied to the surface  
 $\gamma$  = bulk density of the soil

At  $x = X$  the pore pressure is

$$P_w(X,t) = u(X,t) + \gamma_w X \quad [11]$$

And therefore the effective stress is

$$\sigma'(X,t) = P_0 + \gamma' X - u(X,t) \quad [12]$$

Where  $\gamma'$  = submerged density of the soil

$$\Delta\sigma' = \sigma'(X, t) - \sigma_0' \quad [13]$$

Where  $\sigma_0'$  = initial effective stress in the soil

It is assumed that in ice-rich soils,  $\sigma_0'$  is zero. Therefore, from Equations [12] and [13]:

$$\Delta\sigma' = P_0 + \gamma' X - u(X, t) \quad [14]$$

From Equations [14] and [9], the following equation is derived:

$$P_0 + \gamma' X - u(X, t) = \frac{c_v \frac{\partial u}{\partial x}(X, t)}{\frac{dX}{dt}} \quad \begin{matrix} x = X(t) \\ t > 0 \end{matrix} \quad [15]$$

Analytical solution:

A solution to [3] subject to the boundary conditions expressed by [4], [5] and [15] is assumed in the form:

$$u(x, t) = A \operatorname{erf}\left(\frac{x}{2\sqrt{c_v t}}\right) + Bx \quad [16]$$

Where  $\operatorname{erf}(\ )$  = error function

The constants A and B may be found from the boundary conditions and are:

$$A = \frac{P_0}{\operatorname{erf}(R) + \frac{e^{-R^2}}{\sqrt{\pi} R}} \quad [17]$$

$$B = \frac{\gamma'}{1 + \frac{1}{2R^2}} \quad [18]$$

Where  $R = \frac{\alpha}{2\sqrt{c_v}}$  = thaw consolidation ratio

Therefore the complete solution is:

$$u(x,t) = \frac{P_0}{\operatorname{erf}(R) + \frac{e^{-R^2}}{\sqrt{\pi}R}} * \operatorname{erf}\left(\frac{x}{2\sqrt{c_v t}}\right) + \frac{\gamma' x}{1 + \frac{1}{2R^2}} \quad [19]$$

It is convenient to introduce the dimensionless variables:

$$z = \frac{x}{X(t)} \quad \text{and} \quad W_r = \frac{\gamma' X(t)}{P_0} \quad [20]$$

[19] becomes:

$$u(z,t) = \frac{u(z,t)}{P_0 + \gamma' X} = \left(\frac{1}{1 + W_r}\right) \frac{\operatorname{erf}(RZ)}{\operatorname{erf}(R) + \frac{e^{-R^2}}{\sqrt{\pi}R}} + \frac{z}{\left(1 + \frac{1}{2R^2}\right)\left(1 + \frac{1}{W_r}\right)} \quad [21]$$

Where  $W_r$  = measure of the relative magnitude of the applied load and the effective overburden pressure at the thaw line

For a weightless material ( $W_r=0$ ):

$$\frac{u(z,t)}{P_0} = \frac{\text{erf}(RZ)}{\text{erf}(R) + \frac{e^{-R^2}}{\sqrt{\pi}R}} \quad [22]$$

For a soil consolidating under its own weight ( $W_r=\infty$ ):

$$\frac{u(z,t)}{\gamma'X} = \frac{Z}{\left(1 + \frac{1}{2R^2}\right)} \quad [23]$$